Materials Engineering for Enhanced Tissue Scaffold Mechanical Properties

Thesis

Presented in Partial Fulfillment of the Requirements for the Degree Master of Science in the Graduate School of The Ohio State University

By

Jason W. Drexler, B.S.

Materials Science and Engineering Graduate Program

The Ohio State University

2010

Thesis Committee:

Dr. Heather M. Powell, Advisor

Dr. John Lannutti

Abstract

As the body's natural scaffolding is largely comprised of collagen, a significant amount of research is being conducted focused on how to engineer collagen scaffolds with properties identical to natively derived collagen. A major benefit of utilizing collagen as the source material for tissue engineering scaffolds is its bioactive chemistry and ability to support cell attachment and growth. Currently, the only commercially successful tissue engineered product, Apligraf®, utilized a collagen scaffolds to form temporary skin. Despite the benefits of collagen-based tissue engineering scaffolds, many challenges are associated with the use of these materials including low strength, low stiffness and long processing times.

This study utilized two materials design approaches to control tissue engineering scaffold mechanics while maintaining the advantageous biological properties of the scaffold. Crosslinking and coaxial electrospinning were utilized to increase collagen scaffold strength, control protein scaffold stiffness, and to control engineered tissue strength. Physical crosslinking of electrospun collagen using dehydrothermal (DHT) treatment was investigated to decrease processing times while increasing the scaffold strength. The efficacy of *in situ* crosslinking of collagen was also investigated to ascertain whether post-spinning crosslinking could be avoided. Finally coaxial electrospinning was utilized to control the mechanical properties of a gelatin scaffold and the ability of this scaffold type to increase the mechanical properties of engineered tissue was investigated.

All methods employed in these studies, *in situ* crosslinking, DHT treatment, and coaxial electrospinning, significantly increased the strength of tissue engineering scaffolds. Similarly, every scaffold in this study was able to support human cells within the respective 3D structure. The additional advantage of the scaffolds produced using the coaxial electrospinning process was the ability to control the observed mechanical properties including ultimate tensile strength (UTS) and stiffness. Comparatively the *in situ* crosslinking method had a low strength which was not significantly different than the DHT treated scaffold and was significantly lower than post-spinning crosslinking with EDC. Based on these results it was determined that *in situ* crosslinking was not suitable for use in skin tissue engineering scaffolds. While DHT had similar strength as *in situ* crosslinking, this method did not require chemical treatments and therefore had a significant advantage over chemical crosslinking. The addition of a PCL core to a gelatin fiber had the most significant impact on strength in this study. While the pure gelatin scaffold had a UTS of 223.06±43.58 kPa the coaxial scaffolds ranged in strength from 361.91±114.76 to 623.17±87.26 kPa. Similarly the stiffness of the gelatin was increased from 338.82±67.01 kPa in the gelatin to 1,613.82±670.29 kPa in the coaxial scaffold with the largest core diameter. Engineered skin grown on the coaxial scaffolds was also shown to have significantly greater UTS than the skin grown on the gelatin scaffolds. While *in situ* crosslinking did not perform as expected, DHT crosslinking and coaxial electrospinning showed promise for use in tissue engineering scaffold stabilization.

Dedication

This thesis is dedicated to my wife Julie and my family who provided support, motivation and inspiration throughout my studies.

Acknowledgments

This thesis would not have been possible without the support and guidance of Dr. Heather Powell who has been an exceptional advisor during my time at The Ohio State University. I would like to thank my committee member Dr. Lannutti and the members of the Powell lab for advice and support.

Vita

2008	B.S. Materials Science and Engineering, Washington State University
2008 to present	Graduate Research Associate, Department of Materials Science and Engineering, The Ohio State University

Fields of Study

Major Field: Materials Science and Engineering

Table of Contents

List of Tables

List of Figures

Chapter 1: Introduction

1.1 Tissue Engineering

Tissue engineering has the potential to repair or replace diseased and damaged tissue without the need for organ donors. Currently, the extreme imbalance between suitable donor organs and transplant patients have left more than 100,000 people waiting for organ transplants [1] with 19 people dying everyday [2] while on an organ transplant waitlist. Even if a patient receives a tissue transplant there is a large risk of transplant rejection and disease transfer [3]. Tissue engineering could be utilized to develop autologous organ replacements that would avoid the risk of transplant rejection and disease transfer as the engineered tissue would be derived from the patients own tissue. While the field is nowhere near the ability to replace all the functions of complex organs, there have been significant advancements in the technology.

Within the United States approximately 500,000 people receive treatments for burn injuries every year, with 40,000 hospitalizations, 25,000 admissions to hospitals with specialized burn centers, and an estimated 4,000 mortalities [4]. Conventional treatments for full thickness burns involve the use of split-thickness skin autografts and donor skin harvesting [5]. The mortality of these patients is closely related to the percentage of total burn surface area (TBSA) [6]. Therefore burns covering a large portion of the skin limit the available donor sites for autografts and prevent rapid wound closure. Tissue engineered skin has the advantage of reduced size of the donor site

required to cover the same portion of the wound as a split thickness autograft (Figure 1.1) [7].

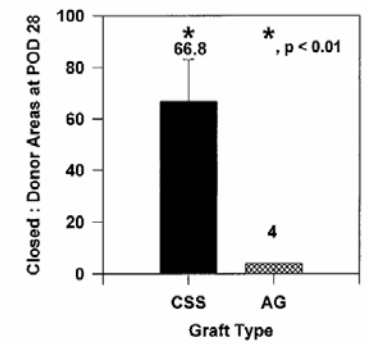

Figure 1.1. Plot of closed donor areas at post operation day (POD) 28 versus the type of graft including cultured skin substitute (CSS) and autograft (AG). Image from Boyce et al. [8].

Several types of tissue engineering grafts exist as well as methods for preparing the grafts. Epidermal autografts are prepared by harvesting epidermal keratinocytes from the patient, culturing them *in vitro*, and grafting this onto the patient [9]. This type of graft lacks a dermal constituent which is linked to graft failure due to poor attachment to the wound surface [9]. Another method of creating engineered tissue that is commercially available, called Integra®, uses a bovine collagen scaffold bonded to a silicone sheet [3,10]. The patient's own cells are seeded onto the collagen which is placed on the patient to promote dermal growth [3]. After removal of the silicone sheet, a thin epidermal

autograft is applied [3]. Nguyen et al. found that after one year the elastic properties of skin treated with the skin substitute were comparable to the patient's untreated skin [11]. However, other studies using this skin substitute observed graft failure due to infection [3]. Another form of engineered tissue, autologous cultured skin substitutes, are formed by culturing a dermal-epidermal composite on a biodegradable collagen scaffold using the patient's own cells and grafting this onto the patient's wound [5,8]. Using this method the engineered tissue did not perform as well as the autograft; however the percentage of healed donor sites was higher for the engineered skin versus the autograft after 28 days of healing (Figure 1.1) [3]. These studies demonstrate the potential benefits of engineered tissue and also demonstrate room for improvement with the technology.

Engineered human skin is formed by the inoculation of cells onto a temporary scaffold *in vitro*, allowing the tissue to develop *in vitro*, followed by transplantation *in vivo*. While tissue engineering is a very promising method for treating failing tissue and organs there is significant room for improvement in all aspects of the process. Specifically, tissue formation is time consuming, requiring about 2 weeks prior to grafting [8] and the tissues grown using the process are weak and fail prematurely [12]. Scaffold design is extremely important since the structural, chemical, and mechanical features of the material will influence the development of the tissue and the overall properties of the tissue. Current tissue engineering technology cannot produce scaffolds or engineered tissue that has the same properties as native human tissue [13]. Improving

upon scaffold design is an important engineering consideration for tissue engineering to succeed.

1.2 Scaffolds for Tissue Engineering

The scaffolds used in tissue engineering are designed to mimic the structural, chemical and mechanical properties of the bodies' natural extracellular matrix (ECM). The ECM is made up of anisotropic nanometer diameter protein fibers primarily composed of protein from the collagen family [14]. Collagen fibers within the ECM are interwoven in a hydrated network of glycosaminoglycan chains and elastin fibers [15].This network of fibers not only supports the tissue mechanically, it is responsible for transferring external mechanical stimuli to the cell which the cell uses to produce molecular signals [16,17]. Tissue engineering scaffolds are fabricated using methods that attempt to reproduce the structural features of the ECM specifically, nanometer diameter fibers and an interconnected pore network. Beyond the structural requirements, scaffolds must maintain appropriate chemistry for cell-scaffold interaction, mechanical integrity, biocompatibility, and ideal degradation at a rate comparable to native ECM production to allow for replacement of the temporary scaffold without loss in function [39,40]. Several manufacturing methods exist to produce scaffolds that mimic the ECM including fiber bonding [18], phase separation [18,19], solvent casting [18,20], particulate leaching [18,20], extrusion [18,21,22], and freeze drying [18,23]. Other common techniques

include the formation of hydrogels [24] and electrospinning of polymer nanofibers [25]. While all the techniques mentioned have potential for manufacturing of tissue engineering scaffolds, electrospinning is one of the most promising methods for scaffold fabrication because it can economically produce scaffolds out of a wide range of materials with architectural and chemical features similar to native ECM.

Electrospinning produces a randomly oriented polymer fiber matrix with fiber diameters that range from hundreds of nanometers to tens of micrometers. The process of electrospinning is performed by applying a voltage to the outlet of a syringe needle containing a polymer solution (Figure 1.2). The applied voltage creates an electric field between the needle outlet and a grounded metal collector. As a droplet of solution forms at the needle tip, positive and negative ions within the solution begin to move in opposite directions based on the applied electric field, putting a force on the droplet, and once surface tension is overcome a jet of polymer solution is produced [26]. The forces acting on the jet propel it towards the grounded collector as the polymer is stretched into a thin fiber. During this process, solvent evaporates from the fiber, thinning it out further and eventually leading to a solid, randomly oriented, polymer fiber matrix deposited on the collector. The final diameter of the fibers collected depends on solution concentration, flow rate, solvent, and the surface tension of the polymer solution [27]. This process is attractive since it is an inexpensive technique, scale-up is possible and a range of polymers can be produced including both synthetic and natural polymers.

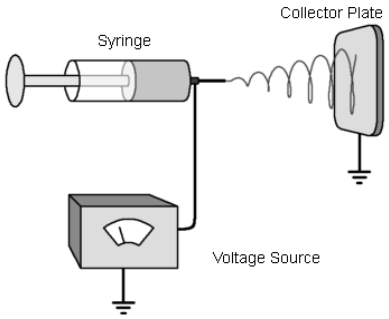

Figure 1.2. Example of an electrospinning setup. Image from [28].

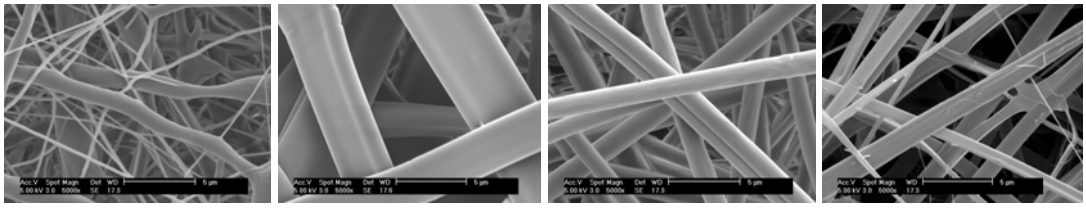

Figure 1.3. Scanning electron micrographs of electrospun fibers including (from left to right) polycaprolactone (PCL), gelatin, a blend of gelatin and PCL and collagen. Scale bar = 5μm.

A variety of materials are used for electrospun tissue engineering scaffolds. Some popular synthetic materials include poly(lactic acid) [29-31], poly(glycolic acid) [29-31], poly(ethylene oxide) [29,30], poly(vinyl alcohol) [29,30], poly(acrylic acid) [29,30], polydioxanone [31], and poly(ε-caprolactone) (PCL) [29-31]. Copolymers such as poly(lactide-*co*-glycolide) (PLGA) have also been produced via electrospinning to form

scaffolds for tissue engineering [32]. A synthetic PLGA electrospun scaffold was shown to promote human mesenchymal stem cell attachment, growth and proliferation while maintaining phenotypic shape [32]. The alternative to synthetic polymers is naturally derived polymers. Several naturally derived polymers used for tissue scaffolds include chitosan [29,30,33], collagen [22,33-36], fibrinogen [37], and gelatin [35,38]. Electrospun collagen and gelatin have been utilized for the production of engineered skin with well stratified dermal and epidermal components [39,40]. Electrospun gelatin scaffolds have been shown to support tissue formation and variations in interfiber distance (Figure 1.3) using different scaffolds demonstrated that an interfiber distance of 5-10μm in electrospun gelatin scaffolds promoted optimal tissue formation *in vitro* [40]. Collagen nanofibers were also shown to support the formation of engineered skin as well as maintain high levels of engraftment; the scaffold reduced wound contraction when compared with a freeze-dried collagen sponge [39].

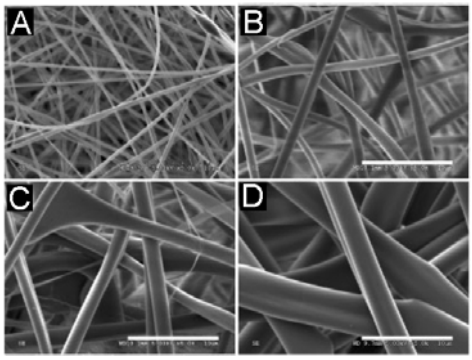

Figure 1.4. Scanning electron micrographs of electrospun gelatin fibers with varying fiber diameter and interfiber distance. Fiber diameter and interfiber distance increases from A to D. Scale bar = 10μm. Image from Powell and Boyce [40].

Tissue engineering scaffolds must be designed with the target organ in mind in order to develop a suitable tissue replacement. Structural features of the scaffold are extremely important for regulating tissue growth and this will change between different tissues. For example, a scaffold that is appropriate for engineered skin may not be suitable for a heart valve replacement. As demonstrated by Powell and Boyce electrospinning has the versatility to adjust structural features of the scaffolds to optimize tissue development and therefore create an ideal tissue replacement [40].

1.3 Mechanical Properties of Tissue Engineering Scaffolds

Scaffold mechanics are an extremely important factor in tissue engineering scaffold design. Scaffold mechanics dictate the health and phenotype of the constituent cells and can control the mechanical properties of the resultant tissue. In native human

tissue the ECM provides mechanical integrity to the tissue [15]. Since scaffolds are intended to be a temporary extracellular matrix, these scaffolds must also provide mechanical support to the tissue *in vitro* and *in vivo* until full integration or remodeling has occurred. If the engineered tissue is not designed with the proper strength, it is susceptible to failure during implantation or shortly thereafter. These problems are common within the tissue engineering community as engineered tissues generally have significantly lower strength than their native human counterparts [13]. The stiffness of a scaffold is also an important design consideration for tissue engineering scaffolds since it has been shown to regulate many cellular behaviors including cell-matrix adhesions and size of the focal adhesions [41,42], motility [43,44], propagation [45], differentiation [46-48], viability [48], phenotype [47,49] and apoptosis [50]. Scaffold mechanics are therefore extremely important as they provide temporary strength and they guide cellular behaviors.

While there are methods of fabricating scaffolds for tissue engineering that mimic the architectural and chemical features of the ECM, there are no methods for creating scaffolds that are similar in strength and stiffness to the ECM [13]. For example collagen has low mechanical strength and often degrades with exposure to water despite the fact that collagen is derived from natural sources [51]. The methods used to isolate collagen from the source, degrades the structural features of the collagen causing a reduced load bearing capacity of the scaffolds from which this material is made. To address these issues several methods including chemical crosslinking, copolymerization, and polymer

blending have been employed to improve tissue strength via improved scaffold mechanics.

1.4 Modification of Scaffold Mechanics

The ECM is primarily composed of collagen and, as a result, collagen is the most widely utilized natural polymer for tissue engineering as it mimics both chemistry and molecular interactions with cells [23,52,53]. Unfortunately, synthetically fabricated collagen scaffolds are significantly weaker than naturally derived collagen scaffolds i.e. decellularized dermis [54]. Similarly, collagen has significantly lower strength than synthetic polymers which limits its utility as a scaffold material [12]. To improve collagen scaffold strength and stability, crosslinking is commonly used [55,56]. Both physical and chemical crosslinking methods have been employed to stabilize protein scaffolds for use in aqueous environments.

Physical crosslinking of protein scaffolds is a rapid method of stabilizing and increasing the strength of collagen scaffolds. Methods of physical crosslinking include dehydrothermal (DHT) [34,57] and UV [34,57,58] crosslinking. Collagen has been crosslinked by DHT and UV crosslinking; both methods have been shown to stabilize the collagen *in vitro* [34,57] and no cytotoxic response was observed for either method *in vitro* [57]. However, UV crosslinking works based on light penetration into the scaffold; therefore, the crosslinking of a 3D collagen scaffold is limited in crosslinking extent.

Numerous studies have been performed which utilize DHT stabilization of collagenous natural materials and collagen scaffolds with the use of DHT crosslinking [57,59-65]. During DHT crosslinking, new ester and amide bonds are formed [60,66] leading to significant increases in the strength of collagen compared to non-crosslinked collagen materials [51] and reduced degradation rates upon exposure to collagenase [34]. Fibrous, insoluble collagen crosslinked using DHT crosslinking has also been shown to support cell proliferation and tissue formation [39,51,64]. Despite the positive benefits, DHT crosslinking has not been studied in electrospun collagen which could significantly benefit from one step crosslinking methods performed while the scaffold is dry. This would provide new options for scaffold sterilization and scaffolds could be shipped across the country.

Chemical crosslinking is the most widely used method of crosslinking collagenous tissue engineering scaffolds. Several different chemicals have been used including glutaraldehyde (GA) [36,67,68], hexamethylene diisocyanate (HMDIC) [22,35,57,58] and N-(3-dimethylaminopropyl)-N'-ethylcarbodiimide hydrochloride (EDC) [39,58,69]. Despite the broad utilization of GA as a crosslinking agent, it has been associated with graft failure due to cytotoxicity and calcification [70]. HMDIC has also been shown to cause cytotoxicity due to un-reacted pendant molecules [57,71]. Crosslinking of electrospun collagen with EDC reduced scaffold degradation [59,72], maintained cell viability [73] and has been used successfully to crosslink scaffolds used for bioengineered skin [39], bone [58,74], and cartilage [75]. Collagen crosslinked with

EDC has also been shown to have an increased strength and denaturation temperature compared to similar crosslinking agents [76] due to the formation of new amide and ester bond crosslinks [77]. At low concentrations of EDC, 5mM or lower, the strength of the tissue replacement was significantly improved over uncrosslinked scaffolds [23]. However, EDC crosslinking has been associated with cytotoxicity and reduced tissue strength at concentrations of 10mM or greater [23] and often requires a lengthy rinsing procedure, up to four days, to ensure no crosslinker remains within the scaffold [39,40,78].

Crosslinking is very useful for stabilizing collagen tissue engineering scaffolds. Several methods have been demonstrated to increase the strength and resistance to degradation of these scaffolds. However, almost every crosslinker has been shown to elicit a cytotoxic response especially at high concentrations. Therefore, the extent to which strength and stiffness can be modified is limited. Other methods of controlling scaffold strength and stiffness may be necessary such as the use of a synthetic polymer scaffold or composite scaffolds.

1.4.1 Scaffold Chemistry

Since the ECM imparts a significant amount of strength to native human tissue such as skin, tissue engineering scaffolds need to have similar strength as the native ECM. The most advantageous aspects of synthetic polymers are their high strength and the ability to form them into ECM-like architectures. This means synthetic polymers are widely used in tissue engineering to synthesize scaffolds and their properties can be

customized for different applications. While synthetic scaffolds have the advantage of high strength; they often lack the ability to promote cell attachment and proliferation. Khor et al found that keratinocytes only spread across 36% of the surface of a PCL film on which the cells were coated [79]. Similarly, Venugopal et al found that fibroblast proliferation was significantly lower on PCL than on collagen scaffolds [80].Another study found that chitosan coated poly(lactide-co-glycolide) (PLGA) electrospun fibers had better cytocompatibility than PLGA scaffolds alone [81]. Despite the very attractive mechanical properties, ability to form the scaffolds into specific structures, and resistance to degradation synthetic polymers are at a disadvantage when it comes to cell-scaffold interactions and tissue formation.

1.4.2 Scaffold Blending

One common method of increasing the strength of natural polymer scaffolds while maintaining biocompatibility is to use a combination of natural and synthetic polymers. By using both materials the scaffold would have the benefit of high strength and bioactive properties. Blends have been created and studied by mixing two different polymer solutions and electrospinning the resultant mixture followed by cell culture to determine the scaffold's ability to promote tissue formation [12,38,82-84]. Powell et al. studied the influence of increasing PCL concentration on the mechanical and biological properties of electrospun collagen-PCL blends [12]. It was found that small additions of PCL equal to or greater than 10% significantly increased the strength of acellular hydrated scaffolds [12]. Tissue formed when grown on blended scaffolds had poorly

developed morphology, proliferation was reduced, and the final strength was not significantly different than tissue grown on similar collagen scaffolds [12]. This was believed to be caused by segregation of PCL domains within the blend, leading to cell-PCL interaction and decreased cell affinity for the nanofibers [12]. Scaffolds should have a continuous protein-cell interface for optimum epidermal differentiation.

1.4.3 Composite Scaffolds

Since the cell scaffold interface should consist entirely of cell-protein interactions, methods of containing a synthetic polymer core within a gelatin shell have been proposed. Two potential methods include protein coatings of electrospun nanofibers and coaxial electrospinning. Coatings are made by electrospinning a specific fiber architecture and coating the scaffold with the protein. A protein coating applied to electrospun synthetic fibers has been used to create scaffolds with a bioactive protein shell and a strong synthetic core for tissue engineering [38,85,86]. One method for coating collagen on the surface of an electrospun PCL scaffold is to functionalize the surface of electrospun PCL using plasma treatment followed by fixing collagen on the surface of the fibers [85]. Duan et al. found collagen coated PCL to support fibroblast growth and proliferation to be higher than on electrospun PCL scaffolds [85]. Another method used for coating collagen on PCL scaffolds is soaking a PCL scaffold in a solution of collagen in acetic acid [38]. Zhang et al. showed fibroblast proliferation on these collagen coated PCL scaffolds was significantly greater than electrospun PCL but

was lower than on electrospun collagen scaffolds [38]. Lower cellular proliferation combined with reduced scaffold porosity and additional processing steps [38,85] reduces the feasibility of this method for tissue engineering.

Coaxial electrospinning is a new and promising method that can be used to create tissue engineering scaffolds that structurally mimic the ECM, maintain a protein-cell interface, and have the advantage of strong synthetic polymer reinforcement. Essentially this is a method of coating synthetic fibers with a protein shell that is continuous on all fibers, does not influence porosity, and does not require post-processing of the scaffold. Coaxial electrospinning was first performed by Sun et al. [87]. Since then this technique has been used to manufacture core-shell fibers for controlled drug delivery [88,89], tissue engineering [38,90,91], and a variety of other applications [92-94]. A previous study demonstrated that the strength of coaxial PCL core-gelatin shell fiber scaffolds had greater strength than electrospun gelatin scaffolds [90]. Zhang et al. found no difference in the proliferation of fibroblasts on coaxial collagen shell/PCL core nanofibers when compared with 100% collagen nanofibers [38]. They also reported the coaxial fibers promoted fibroblast proliferation significantly better than collagen coated PCL nanofibers [38]. There is great potential for manufacturing strong scaffolds using coaxial electrospinning. However, no one has studied the influence of a strong synthetic polymer core on the ability to control the mechanical properties of tissue engineering scaffolds or the strength of engineered skin.

While tissue engineering scaffolds attempt to reproduce mechanical characteristics of the ECM they fall short. Crosslinking increases the scaffold strength, however, the process is time consuming often requiring a full day to adequately crosslink the scaffold and the crosslinking agent can cause cytotoxicity if used in too high of concentrations. Ideally a one step crosslinking procedure could be used to stabilize the collagen scaffolds. Incorporating synthetic polymers into a natural scaffold is not an ideal solution though encapsulating a synthetic core within a protein shell could have beneficial attributes such as high strength and bioactivity. Protein coatings on synthetic scaffolds will not be suitable for tissue engineering due to the additional processing steps required as well as the reduction in porosity of the scaffold. Coaxial electrospinning is an ideal manufacturing method since continuous synthetic polymer fibers with a protein shell can be electrospun with no time consuming processing steps and no change in scaffold structure. Even with coaxial electrospinning, synthetic polymer is added to the human body; therefore the balance between increased strength and tissue growth promotion must be maintained to reduce the amount of PCL in the scaffold.

Chapter 2: *In Situ*, DHT, and EDC Crosslinking of Electrospun Collagen

2.1 Introduction

Scaffolds for tissue engineering function as a replacement extracellular matrix (ECM) providing a substrate for cellular adhesion and organization. The chemistry and structure of the ECM can regulate cell proliferation, differentiation, and maturation, thus tissue engineering scaffolds should have a strong resemblance to the natural ECM, which is comprised of nanometer diameter protein fibers [15]. Electrospinning is a simple and efficient method utilized to synthesize a network of nanofibers that approximates the structural and biological properties of the ECM [15,32,36]. This method produces a highly porous nonwoven mat with a high surface to volume ratio and porosity [95,96]. Although electrospun collagen and collagen-based scaffolds have been engineered for a variety of biomedical applications [33,97,98], their insufficient mechanical strength and rapid degradation in aqueous environments requires crosslinking steps before the scaffolds can be utilized for tissue regeneration [38,73].

Two methods of crosslinking include physical and chemical stabilization. Physical crosslinking is performed using dehydrothermal (DHT) treatment in a vacuum oven. DHT processing increases the strength and stability of protein scaffolds via the formation of new ester and amide bond crosslinks and this process has the advantage of no chemical agents used during the processing [60,66]. Since there are no chemical agents, the treatments are non-cytotoxic. DHT crosslinking has been shown to support

cell proliferation and tissue formation [39,51,99]. Despite the positive benefits, DHT crosslinking has not been studied in electrospun collagen which could significantly benefit from crosslinking methods performed while the scaffold is dry. This would provide new options for scaffold sterilization and scaffolds could be shipped across the country.

Chemical crosslinking is widely used to crosslink collagenous tissue engineering scaffolds. Crosslinking with EDC is popular since it has been shown to stabilize the scaffold [72], maintain cell viability [73], increased strength [22] and crosslink scaffolds for various engineered tissues [39,58,74]. EDC crosslinking occurs through the formation of amide and ester bond crosslinks [77]. Crosslinking with EDC is limited since it has been associated with cytotoxicity at concentrations greater than 10mM [23] and often requires a lengthy rinsing procedure to completely remove the crosslinker [39,78]. Thus it would be beneficial to directly compare the efficacy of DHT crosslinking versus EDC crosslinking to determine if the use of chemical crosslinking can be avoided to avoid possible degradation during processing, cytotoxicity and to reduce processing times.

Another limitation to the use of EDC crosslinking is the additional steps required for EDC crosslinking that increase the time to prepare a scaffold along with the limited sterilization methods [23,74,94]. As a result, alternate processing methods are needed. Chemical crosslinking during the electrospinning process has been previously performed by adding GA to chitosan electrospinning solutions [100]. *In situ* crosslinking with GA resulted in smaller fiber diameters, no change in solubility in acidic, basic or aqueous

conditions, and a processing time 25 times faster than the original manufacturing method [100]. Thus, the addition of a chemical crosslinker to electrospun collagen solutions may be possible.

The goal of this study was to evaluate the utility of dehydrothermal crosslinking of electrospun type I collagen compared to standard chemical crosslinking and the feasibility and efficacy of *in situ* crosslinking. Additionally, the utility of these crosslinked scaffolds for dermal tissue engineering was examined. Collagen scaffolds were prepared by electrospinning soluble type I collagen with and without EDC. Scaffolds with EDC (*in situ*) were DHT crosslinked or utilized as-spun. Scaffolds without EDC were DHT crosslinked, chemically crosslinked or both DHT and chemically crosslinked. As-spun collagen scaffolds without EDC served as a control for this study. The effects of crosslinking on scaffold architecture, stability, mechanical properties, and cytotoxicity were investigated.

2.2 Materials and Methods

2.2.1 Electrospinning Solutions

Electrospinning solutions were prepared by mixing acid soluble collagen from bovine hide (Kensey Nash; Exton, PA) with 1,1,1,3,3,3-hexafluoro-2-propanol (HFP; Sigma-Aldrich Co., St. Louis, MO) at a concentration of 10 wt./vol.% on a magnetic stir plate for 48 hours. *In Situ* crosslinked scaffold solutions were prepared by adding 71mM

of N-(3-dimethylaminopropyl)-N'-ethylcarbodiimide hydrochloride (EDC; Sigma-Aldrich Co.) to the above solution when the materials were combined.

2.2.2 Collagen Scaffolds

Collagen-HFP solutions were electrospun at a potential of 30kV onto an 8.5 cm^2 grounded plate that was positioned perpendicular to the tip of the needle, at a distance of 20 cm with a flow rate of 4 ml/hr. The as-spun scaffolds were then placed into a vacuum sealed desiccator or dehydrothermally crosslinked (DHT) at 140^oC for 24 hours at 30mm Hg. A subset of these scaffolds were crosslinked in a solution of ethanol and N-(3-dimethylaminopropyl)-N'-ethylcarbodiimide hydrochloride (EDC; Sigma-Aldrich Co.) at a concentration of 5mM EDC in 50ml pure ethanol per scaffold for 24 hours. *In Situ* collagen-HFP solutions were electrospun at a potential of 30kV and at a distance of 20 cm with a flow rate of 5 ml/hr. The as-spun scaffolds were then placed into a vacuum sealed desiccator or DHT crosslinked as described above. The *In Situ* crosslinked scaffolds had an equivalent EDC:collagen ratio by weight as the EDC crosslinked scaffolds. Six different scaffolds were prepared: as-spun collagen (Control), collagen with DHT (DHT), collagen with post-spinning EDC crosslinking (EDC), collagen with DHT and post-spinning EDC crosslinking (DHT+EDC), collagen with *In Situ* EDC crosslinking (*In Situ*), and collagen with *In Situ* EDC crosslinking and DHT (*In Situ*+DHT).

2.2.3 Scanning Electron Microscopy

The morphology of the electrospun collagen scaffolds was examined by scanning electron microscopy (FEI Sirion). Punch biopsies from dry scaffolds were collected, mounted onto aluminum tabs with conductive carbon paint, sputter coated with gold-palladium and imaged in secondary electron mode at 5 kV. Images were collected from each sample and the diameter of at least 100 fibers from each scaffold type was assessed quantitatively via Image J software. To assess any change in scaffold morphology after exposure to an isotonic, aqueous media, scaffolds were incubated in sterile, HEPES buffered solution (HBS) at pH 7.4 for 7 days. Scaffolds were then rinsed 2 X 5 min with phosphate buffered saline (PBS, pH 7.4), dehydrated through a graded alcohol series (50%, 70% ethanol for 5 min followed by 80%, 95%, 100% and 100% for 10 min), and dried in a graded ethanol:hexamethyldisilazane (HMDS; Ted Pella Inc., Redding, CA) series (3:1, 1:1 and 1:3 for 30 min each followed by pure HMDS which evaporated overnight). The dried samples were mounted and examined by scanning electron microscopy as above and fiber diameter was determined by image analysis with Image J.

As electrospun scaffolds have no true pores, the free space between fibers was quantified using interfiber distance. Interfiber distance was calculated by measuring the distance between a fiber and the closest adjacent fiber within the same plane. A minimum of 20 interfiber distances were calculated per sample with six samples per group. Mean interfiber distance ± standard deviation was reported.

2.2.4 Transmission Electron Microscopy

To examine the microstructure of electrospun collagen the as-spun scaffolds were crosslinked using their previously described protocols, rinsed two times with milli-Q water for 1 hour and post-fixed with 1% osmium tetroxide for 1 hour. Next, the collagen scaffolds were rinsed three times with deionized water for 5 minutes each rinse, exposed to a graded ethanol series (50%, 70%, 80%, 95%, 100% and 100% ethanol for 10 min), exposed to 100% hexamethyldisilazane (HMDS) three times for 10 min, and dried overnight in 100% HMDS. Then the samples were trimmed and embedded in epoxy resin followed by sectioning on a Leica EM UC6 ultramicrotome cutting at 100 nm. Sections were examined with a Tecnai G2 Spirit TEM operated at 100 kV. *In Situ* and *In Situ*+DHT samples were not investigated using this method as discussed later.

2.2.5 Tensile Testing

The mechanical properties of collagen scaffolds were quantified via tensile testing (n = 6 per group). Scaffolds were re-hydrated with HBS and punched into dogbone-shaped specimens with a gauge length of 20 mm and width of 4 mm. The specimens were mounted into the grips of a tensile tester (TestResources 100R; Shakopee, MN) with a 10N load cell and tested to failure at a strain rate of 2 mm/sec to avoid specimen dehydration during testing. Data from samples which did not break within the gauge length were discarded. Ultimate tensile strength (UTS) was measured and reported as mean $\pm$ standard deviation. Stiffness was measured as the slope within the linear region of the stress-strain curve and reported as mean $\pm$ standard deviation.

2.2.6 Scaffold Stability

The biostability of the collagen scaffolds was evaluated via exposure to collagenase of bacterial origin (collagenase type I; Worthington Biochemica Corp., Lakewood, NJ). Dry scaffolds were punched into 18 mm diameter circles (n = 6 per group), weighed, sterilized in 70% EtOH, placed into a 12-well plate with media containing 1 U/ml collagenase per mg of collagen and incubated at 37ºC and 5% CO_2 for 3 days. Collagen content in the media was assessed at 1, 3, 6, 24, and 72 hours using a hydroxyproline assay [23]. Because the matrices contain type I collagen plus an unknown amount of carbohydrates and lipids a standard curve was generated by testing the absorbance of known quantities of a raw collagen material. Collagen content in experimental samples was extrapolated using the standard curve within the linear region.

2.2.7 Fourier Transform Infrared Spectroscopy

Infrared spectra of the electrospun collagen scaffolds were obtained using the attenuated total reflectance (ATR) mode of a Nicolet Nexus 670 benchtop FTIR spectrometer with a continuum microIR microscope (Thermo Scientific; Waltham, MA). A germanium crystal was used for the ATR analysis. Spectra were obtained between the wave numbers of 600-4000cm^{-1} and were normalized to the methyl peak at 2950cm^{-1}. The extent of crosslinking was compared between samples by measuring the peak height at 1546cm^{-1} which indicates the formation of amide bonds and at 1100 cm^{-1} indicative of ester bonds. *In Situ* and *In Situ*+DHT samples were not investigated using this method.

2.2.8 Cellular Interaction: Viability and Penetration

The toxicity of the crosslinking procedure was determined by assessing the cellular viability of fibroblasts cultured on the scaffold for 7 days. Human primary dermal fibroblasts were inoculated into the scaffolds at a density of $1x10^6$ cells/cm^2. Fibroblasts were cultured for a total of 7 days with 4 mm punch biopsies removed from the scaffold at 1, 3, 5, and 7 days (n = 6 per group, n = 6 per time point). A MTT assay was performed on the punch biopsies immediately after collection following a protocol previously described [40]. Briefly, 0.5 ml of a sterile filtered solution of 0.5 mg MTT/ml PBS solution was added to each well of a 24-well plate, each containing one 4 mm punch. The biopsies were incubated in the MTT solution for 3 hours at 37ºC and 5% CO_2. After three hours, the MTT solution was aspirated from the well and replaced with 0.5 ml methoyxyethanol (Fisher Scientific; Fair Lawn, NJ) and agitated on a rocking plate for 3 hours to dissolve the formazan crystals. The amount of MTT-formazan product released was measured at 590 nm on a microplate reader with values reported as mean optical density $\pm$ standard deviation.

To determine the penetration depth of cells into scaffolds, 8 μm thick sections of the samples cultured with fibroblasts for 7 days were mounted and stained with propidium iodide (cell nuclei) and rabbit anti-collagen type I (Santa Cruz Biotechnology). Samples were characterized using a laser scanning confocal microscope (Zeiss LSM 510 Meta). Measurements of cell penetration depth (n = 5 per location, n = 5 per condition) were obtained using the Zeiss Image Browser software.

2.2.9 Statistical Analyses

All data was analyzed using SigmaStat 3.10 (Systat Software Inc; San Jose CA). Differences between the groups were analyzed using Student's t-tests. P values less than 0.05 were considered statistically significant.

2.3 Results

2.3.1 Scaffold Structure

Collagen scaffolds were comprised of randomly oriented, ribbon-like fibers 1.59 ± 0.60μm in diameter (Figure 2.1A and Figure 2.2E). Exposure to dehydrothermal (DHT) crosslinking maintained the as-spun fiber morphology with no change in fiber diameter or interfiber distance (Figure 2.1B and Figure 2.2A & E). The addition of the crosslinker, EDC, to the electrospinning solution did not alter its ability to be electrospun. A scaffold of continuous fibers was generated with all solutions. *In Situ* crosslinking with EDC significantly altered the structure of the collagen scaffolds generating thinner, more rounded fibers compared to control and DHT scaffolds (Figure 1).

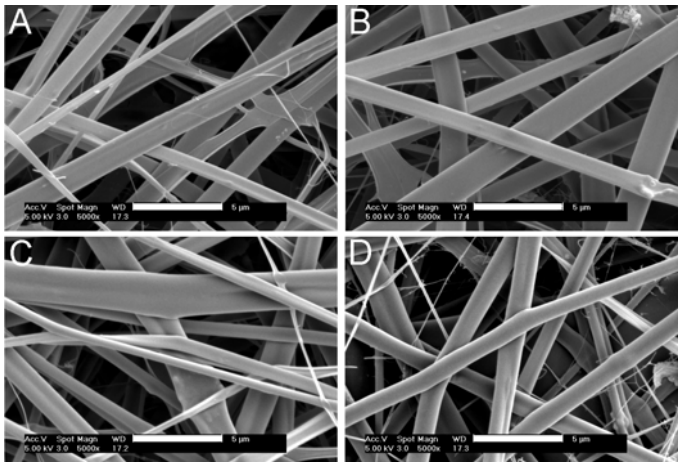

Figure 2.1. Scanning electron micrographs of electrospun collagen scaffolds. A) as-spun collagen (Control), B) as-spun collagen with dehydrothermal crosslinking (DHT), C) as-spun *In Situ* EDC crosslinked (*In Situ*), and D) as-spun *In Situ* crosslinked with DHT (*In Situ*+DHT). Note thinner fibers in *In Situ* and *In Situ*+DHT groups. Scale bar = 5µm.

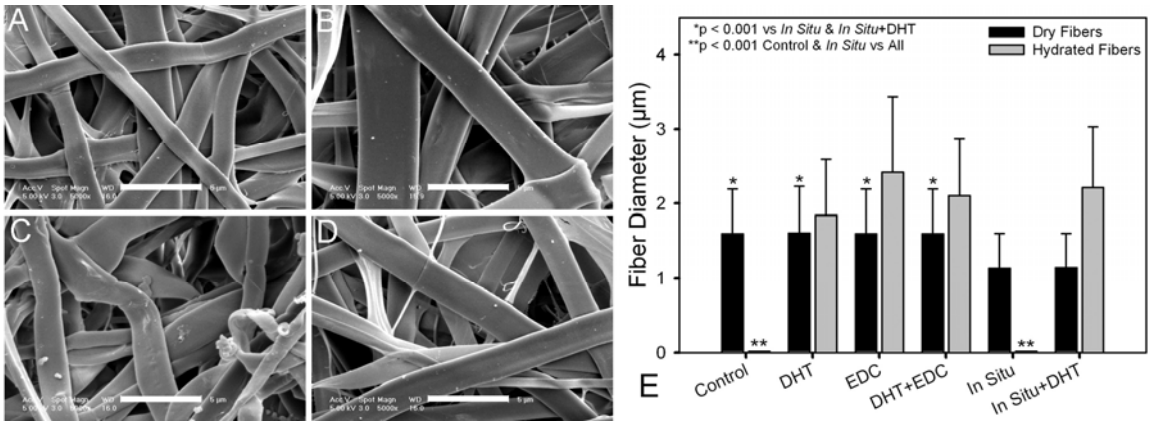

Figure 2.2. Scanning electron micrographs of A) DHT, B) EDC, C) DHT+EDC, and D) *In Situ*+DHT after incubation in Hepes buffered saline for 7 days. E) Fiber diameters of as-spun (dry) and hydrated scaffolds. Dry control scaffold measurements used to compare with EDC and DHT+EDC respectively. All fiber diameters significantly different intra group ($p<0.05$). Control and *In Situ* scaffolds completely degraded by day 7. Scale bar = 5µm.

After incubation in HBS for 7 days, the control and *In Situ* groups completely degraded while the DHT, EDC, DHT+EDC, and *In Situ*+DHT groups remained intact and were characterized by larger fiber diameters (Figure 2.2A-D). Quantification of fiber diameter confirmed these results with the *In Situ*+DHT group experiencing the greatest increase in fiber diameter after hydration while the fibers within the DHT group increased the least (Figure 2.2E). Fibers crosslinked with EDC only experienced fiber swelling after hydration with a 50% increase in fiber diameter while the fibers with DHT crosslinking increased by 15% on average (Figure 2.2E). Transmission electron microscopy confirmed the fiber morphology observed in SEM; however no samples displayed the 67nm banding that is characteristic of native collagen as seen previously with electrospun collagen [36] (Figure 2.3). Control scaffolds degraded during processing thus no TEM imaging could be conducted on these samples.

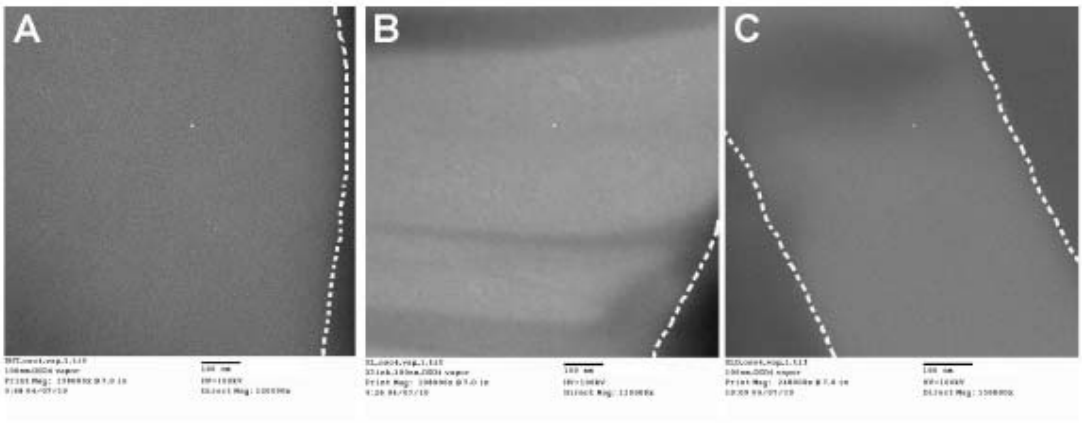

Figure 2.3. Transmission electron micrographs of OsO_4 stained and sectioned electrospun collagen fibers crosslinked using A) DHT, B) EDC, and C) DHT+EDC. Control scaffolds degraded during processing. The white dashed line indicates the fiber edge. Scale bar = 100nm.

2.3.2 Scaffold Stability

As the stability of a scaffold is important for manipulation during cell inoculation and subsequent tissue engineering operations, the degradation rate of scaffolds is extremely important. All scaffolds exposed to bacterial collagenase showed signs of degradation (Figure 2.4). The *In Situ* group had the greatest rate of degradation compared to the other groups with close to 95% degradation after 6 hours of exposure to collagenase (Figure 2.4). Similar to the *In Situ* samples, the control samples rapidly lost mechanical integrity and fragments after approximately 3 hours exposure (data not shown). A hydroxyproline assay was used to quantify the amount of degraded collagen found within the medium and confirmed the visual observation that the non-crosslinked

Control group had the second most rapid degradation rate after *In Situ* (Figure 2.4). After 24 hours of collagenase exposure, the Control group was 89.95 ± 10.15% degraded whereas the DHT and EDC crosslinked samples were 69.07 ± 14.15%, and 62.37 ± 12.22% degraded respectively. The DHT+EDC sample was significantly less degraded than all other groups, with the DHT and EDC groups significantly less degraded than control but not statistically different than one another (Figure 2.4). After 72 hours of exposure, no Control or *In Situ* scaffolds were visible; however the DHT+EDC and *In Situ*+DHT scaffolds maintained their integrity with 45.05 ± 7.34% and 20.92 ± 2.71% of the scaffolds degraded respectively (Figure 2.4).

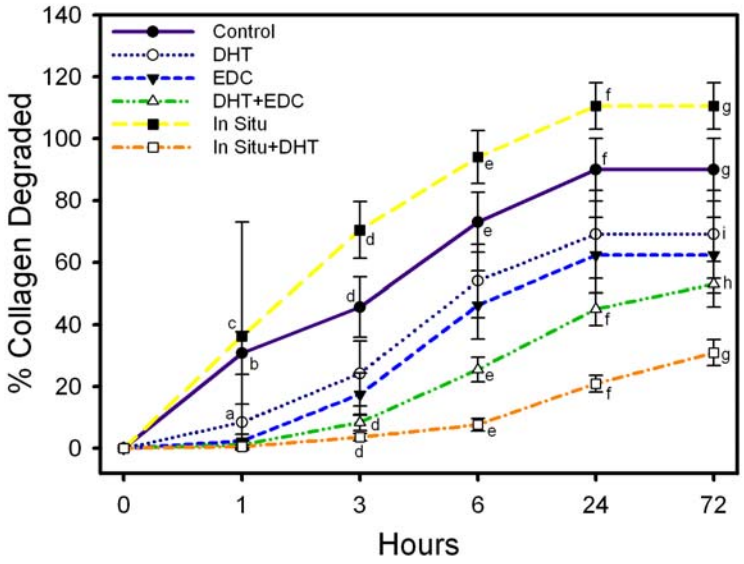

Figure 2.4. Resistance to degradation of collagen scaffolds as a function of crosslinking method when exposed to medium containing 1U/mL collagenase. The percentage of collagen degraded after 1, 3, 6, 24, and 72 hours in solution is shown. [a,d,e,f,g]$p<0.05$ vs All, [b]$p<0.001$ vs DHT, *In Situ*+DHT, EDC, and DHT+EDC, [c]$p<0.001$ vs *In Situ*+DHT, EDC, DHT+EDC, and DHT, [h]$p<0.05$ vs *In Situ*, *In Situ*+DHT, DHT, and Control, and [i]$p<0.05$ vs control, DHT+EDC, *In Situ*, and *In Situ*+DHT.

2.3.3 Scaffold Strength

In addition to maintaining biostability, a scaffold must also maintain sufficient strength for easy manipulation *in vitro*, during surgical application and to reduce failure *in vivo*. The ultimate tensile strength of the scaffolds was highly dependant on crosslinking method. The control and *In Situ* scaffolds degraded and lost all mechanical integrity after hydration thus their mechanical properties could not be quantified. Post-spinning crosslinking with EDC significantly improved scaffold strength compared to *In*

Situ crosslinking in both the DHT and non-DHT groups (Figure 2.5A). Collagen scaffolds crosslinked with DHT significantly improved strength over the control scaffolds but exhibited only 60% of the strength of the EDC crosslinked scaffolds (Figure 2.5A). Utilizing both crosslinking methods (DHT+EDC) resulted in a significant increase in strength ($p < 0.001$) compared to the processes alone. Stiffness followed a similar trend with the DHT+EDC and EDC exhibiting the largest stiffness and DHT alone the smallest (Figure 2.5B). No significant difference between the EDC and DHT+EDC groups was observed (Figure 2.5B).

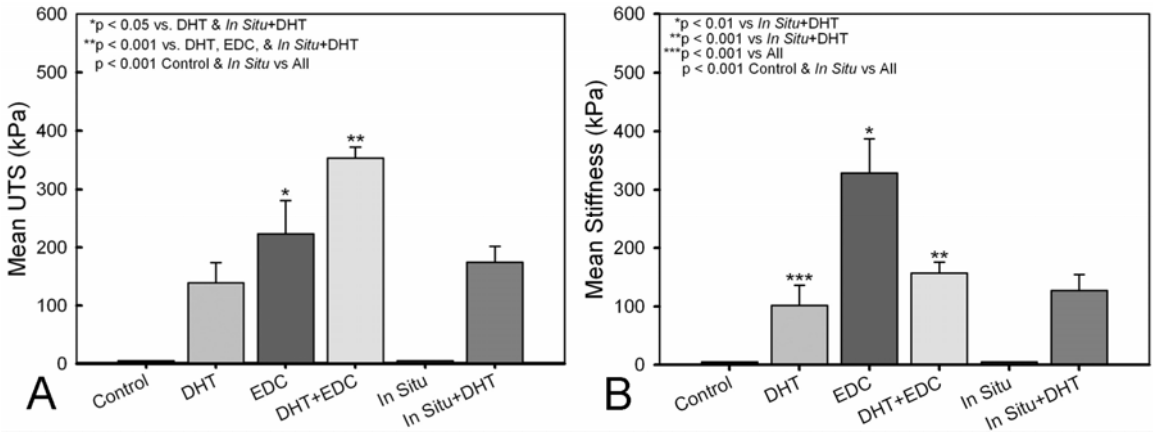

Figure 2.5. Ultimate tensile strength (UTS) of scaffolds (A) and stiffness of scaffolds (B). Control and *In Situ* scaffolds completely degraded before mechanical testing was performed.

2.3.4 Fourier Transform Infrared Spectroscopy

The spectra obtained from the FTIR scans show an increase in peak height at the 1546cm^{-1} wavenumber, which is characteristic of amide bonds [60,69], between the control samples and crosslinked samples (Figure 2.6). The observed peak height increase indicates an increase in the number of amide bonds and crosslinks formed during the reaction [60]. Peak height measurements at 1546cm^{-1} showed that the peak height for EDC crosslinked samples was approximately 45% higher than the Control and 50% shorter than DHT, but very similar to the DHT+EDC crosslinked sample (Figure 2.6). An analysis of ester bond formation at wave number 1100cm^{-1} was attempted however the peaks were too small to observe any significant trends. FTIR was not performed on *In Situ* or *In Situ*+DHT crosslinked scaffolds.

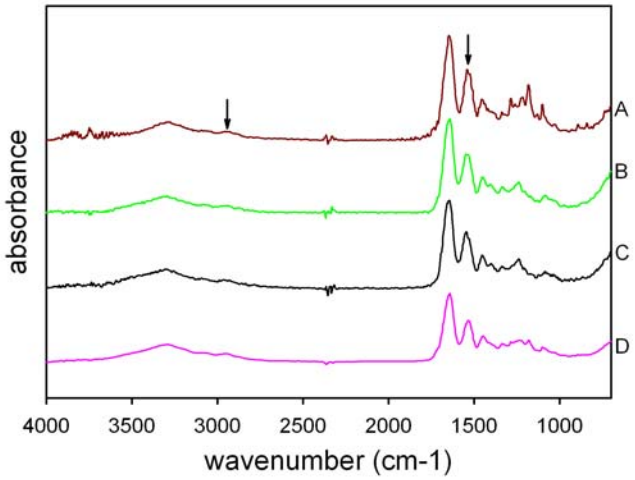

Figure 2.6. FTIR spectra of crosslinked electrospun collagen scaffolds with A) Collagen, B) DHT+EDC, C) EDC, and D) DHT. The arrows indicate the normalization peak at 2950cm^{-1} and amide peak at 1546cm^{-1}.

2.3.5 Cell Adhesion and Viability

Primary human dermal fibroblast viability within these scaffolds was assessed using an MTT assay. The Control scaffold degraded during the sterilization and rinsing process thus no data on cellular behavior within the scaffolds could be obtained. Significantly reduced cell viability was seen at all time points in the DHT group (Figure 2.7). At day 7, the viability of fibroblasts on the DHT scaffolds was on average 13% lower than the viability of the EDC scaffolds and 4% lower than the DHT+EDC group. The EDC and DHT+EDC groups were not statistically different from one another at days 3, 5 and 7 (Figure 2.7).

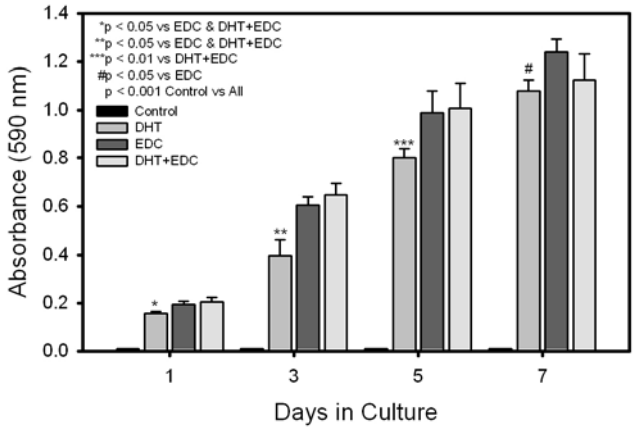

Figure 2.7. Metabolic activity assay (MTT) of fibroblasts cultured on respective scaffolds for 1, 3, 5, and 7 days in culture.

Cellular penetration into the scaffolds was altered by scaffold crosslinking. Cells infiltrated over half of the DHT and DHT+EDC scaffolds at 59.9 ± 6.2% and 56.7 ± 8.8% respectively at culture day 7, and they reach the upper half 49.9 ± 4.8% of the EDC scaffold (Figure 2.8). The differences are not significantly different for the DHT and DHT+EDC scaffolds or the EDC and DHT+EDC scaffolds; however, the penetration of cells into the EDC and DHT were significantly different ($p<0.05$).

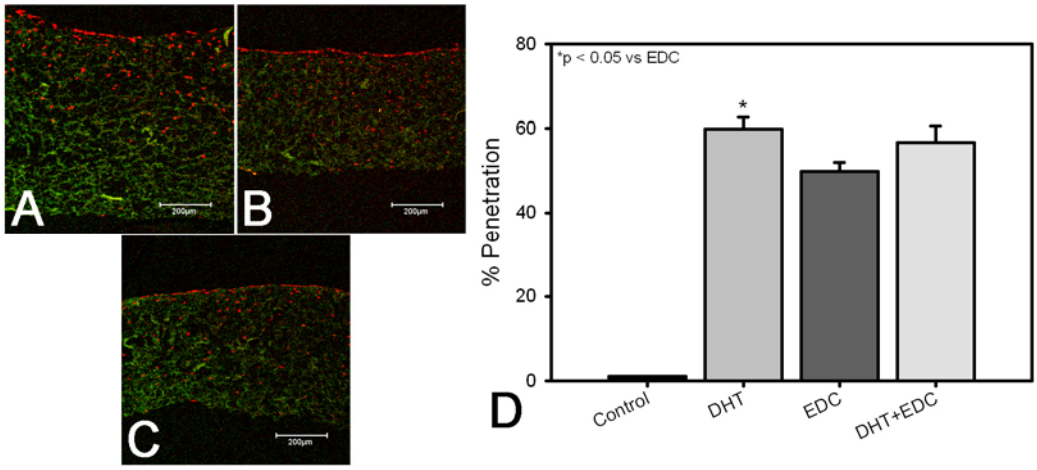

Figure 2.8. Immunostained sections of human dermal fibroblasts cultured on A) DHT, B) EDC, and C) EDC + DHT electrospun collagen scaffolds for 7 days (red = cell nuclei, green = collagen). Scale bar = 200µm. D) Percent penetration of cells into the scaffolds as a function of crosslinking method.

2.4 Discussion

2.4.1 Efficacy of In Situ Crosslinking

In situ electrospinning did not change the ability to electrospin collagen fibers (Figure 2.1). *In situ* crosslinking produced small rounded fibers with smaller fiber diameter than electrospun collagen; however *in situ* crosslinking produced scaffolds (*In Situ)* with the lowest biostability and complete degradation after exposure to HBS for 7 days (Figure 2.2 and Figure 2.4). The addition of DHT crosslinking increased the stability of the scaffold, however the strength and stiffness of the *In Situ*+DHT scaffold was significantly lower than the strength and stiffness of scaffolds crosslinked using traditional EDC in ethanol (Figure 2.5). *In Situ*+DHT fibers also had the greatest increase

in fiber diameter when exposed to aqueous medium (Figure 2.2E). It is believed that the efficacy of the *In Situ* crosslinking method is lower than the post spinning crosslinking method and allows for rapid partial degradation facilitating the large fiber swelling.

It is postulated that *in situ* crosslinking of collagen is far less effective than post spinning crosslinking due to the solvent. It is possible that the EDC reacted with HFP, as seen previously with other carbodiimide molecules [101], preventing extensive amide bond formation between the carboxylic acid and amine groups of the collagen molecules. Without a catalyst, an alcohol functional group will not react with a carbodiimide [102]. Thus, the overall efficacy of the *in situ* crosslinking in HFP is less than crosslinking in pure ethanol, because the EDC will react with the HFP. Also, prior studies have reported changes in EDC crosslinking efficacy based on the solvent for the EDC. Acetone-water blends were shown to increase crosslinking efficiency compared to water alone and compared to 90 vol.% acetone solutions [103]. Since this was contradictory to the intended results of this experiment further study was stopped and the efficacy of DHT, EDC, and DHT+EDC crosslinking was analyzed. While *in situ* crosslinking did not work as mentioned in this study, it does not mean the method is invalid. Processing at lower temperatures or with different solvents could facilitate this production method.

2.4.2 Electrospun Collagen Fiber Morphology

As-spun and DHT crosslinked samples showed no significant difference in morphology (Figure 2.1), fiber diameter (Figure 2.2) or interfiber distance (data not shown). In contrast, EDC crosslinked fibers exhibited the largest increase in fiber

diameter, compared to post spinning crosslinking treatments, whereas the DHT crosslinked fibers experienced minor swelling. It is common for electrospun protein fibers to swell after hydration [38,40]. This phenomenon has been observed before in gelatin nanofibers crosslinked with glutaraldehyde [38]. Protein fiber swelling has been shown to be inversely correlated with crosslink density showing a decrease in swelling with increased crosslink concentration [36,38]. DHT crosslinking has been shown in prior studies to generate lower crosslink densities when compared with chemically crosslinked collagen [58], yet our results indicate that the DHT sample had the least amount of fiber swelling. During dehydrothermal crosslinking, ester and amide bonds are formed reducing the amount of the more hydrophilic free carboxyl, amine, and hydroxyl moieties and leading to more hydrophobic materials as has been previously reported in gelatin scaffolds [104]. Collagen films treated with DHT have also been reported to have slightly greater hydrophobicity than their non-treated counter-parts [105]. In contrast, crosslinking with EDC was not shown to influence collagen film contact angle greatly [105]. The reduced fiber swelling in the DHT crosslinked scaffolds may be a result of increased scaffold hydrophobicity reducing the interaction of the aqueous medium with the fibers.

As DHT crosslinking has been shown to denature collagen molecules [51,58] it was important to investigate the microstructure of the electrospun collagen to determine if they exhibited a banding pattern and if the banding was removed during processing. TEM analysis of the scaffolds indicated that no banding was seen in any of the scaffolds

(Figure 2.3). This is in contrast to previous reports where banding was observed in electrospun type I collagen using the same solvent (HFP) [36]. Collagen fibrils within the non-crosslinked, control scaffolds could not be observed as they degraded during processing. It is possible that the raw material processing denatures the collagen before it is electrospun as the source of type I collagen was different between these two studies. The lack of collagen banding in all samples suggests that denaturation of electrospun collagen during DHT likely further denatures the collagen after electrospinning.

2.4.3 Scaffold Stability and Mechanical Properties

The crosslinking method had a strong influence on the physical properties of the scaffolds. Without crosslinking, collagen fibers rapidly degraded in the presence of aqueous medium (Figure 2.4) and maintained no mechanical integrity. The DHT and EDC scaffolds exhibited similar degradation rates with slightly reduced average degradation in EDC scaffolds, whereas the combination of DHT+EDC was the most stable with approximately 55% of the scaffold remaining after 72 hours of collagenase exposure (Figure 2.4). A greater crosslink density in the EDC samples may have been responsible for its improved biostability when compared to DHT alone. FTIR spectrum indicated an increase in amide bond formation due to EDC crosslinking (Figure 2.6). DHT crosslinking increased the number of amide bonds formed when compared to control scaffolds but reduced these numbers when compared to EDC (Figure 2.6). Previous studies would support the hypothesis that EDC crosslinking is more efficient than DHT crosslinking [59]. Although the combination of DHT and EDC crosslinking

did not significantly improve FTIR peak height compared to EDC alone, the degradation rate of the DHT+EDC samples was significantly lower than DHT or EDC (Figure 2.4). This may be due to a combination of increased amide and ester bond formation as a result of the crosslinking procedures and increased hydrophobicity as a result of the DHT processing. Hydrophobicity of collagen films has been shown to increase after DHT and EDC crosslinking [105].

Mechanical properties of the electrospun collagen scaffolds were improved by all crosslinking methods, however DHT crosslinking was significantly weaker and less stiff than the EDC and DHT+EDC scaffolds (Figure 2.5A). Ultimate tensile strength was significantly improved by using both methods in conjunction with one another whereas no statistical difference in stiffness was observed (Figure 2.5B). The strength of the DHT scaffold was lower than both EDC and DHT+EDC scaffolds which was attributed to lower crosslink density.

2.4.4 Cell-Scaffold Interaction

All scaffolds that did not degrade in aqueous medium were able to support fibroblast attachment and growth. The DHT scaffolds were electrospun, dehydrothermally crosslinked for 24 hours, sterilized for 24 hours then inoculated after approximately 2 hours of rinsing (50 total hours). In contrast, the DHT+EDC samples were electrospun, dehydrothermally crosslinked for 24 hours, chemically crosslinked in EDC for 24 hours, sterilized for 24 hours, rinsed in PBS for 48 hours, then rinsed with HEPES buffered saline for 2 hours prior to inoculation (122 total hours or 2.4X greater

processing time). At days 3, 5 and 7, fibroblast metabolism on the EDC and EDC+DHT scaffolds was not statistically different from one another (Figure 2.7) and on average these scaffolds promoted increased cellular metabolism compared to the DHT group alone. Dehydrothermal crosslinking has been shown to reduce the wetting ability of the scaffolds [105] and may lead to lower seeding efficiency when compared to the EDC crosslinking alone and as a result lower cell number. Cell penetration was also dependant on the scaffold crosslinking method. Fibroblast penetration into the scaffolds was similar for all groups; however it was greater for the DHT and DHT+EDC treated scaffolds. The reduced number of crosslinks could allow fibroblasts to degrade the matrix and migrate within the scaffold with greater ease than a highly crosslinked scaffold.

2.5 Conclusions

Despite the benefit of reduced processing time, stability in collagenase, and ability to support fibroblast proliferation, *In Situ* crosslinking with EDC has a reduced scaffold strength and stiffness and cannot be used without DHT crosslinking. Therefore the method of *In Situ* crosslinking presented here is not suitable for producing scaffolds for tissue engineering and must be modified for future use. Physical crosslinking using dehydrothermal treatment improves mechanical strength and biostability compared to non-crosslinked controls. However, DHT crosslinking appears to produce a lower crosslink density than EDC crosslinked scaffolds resulting in more rapid degradation

rates and reduced strength compared to chemical crosslinking. Dermal fibroblasts adhere and grow on DHT crosslinked scaffolds; but not to the same extent as EDC crosslinked scaffolds. A combination of both processing methods (DHT+EDC) produces scaffolds with the slowest degradation rate and greatest strength but this methods requires 122 hours of post-spinning processing in contrast to a total of 50 hours for DHT. DHT crosslinking can clearly be utilized to stabilize electrospun collagen scaffolds; however one must determine the ideal balance of mechanical properties and processing times for their specific application.

2.6 Acknowledgements

I would like to thank the Campus Microscopy and Imaging Facility at OSU for the use of the confocal microscope and the Campus Electron Optics Facility for the use of the scanning electron microscope. I would also like to thank Jessica Wolever for assistance with the cellular studies.

Chapter 3: Coaxial Electrospinning Control of Core Diameter

3.1 Introduction

Tissue engineering scaffolds are designed to promote tissue growth and organization with the intent to repair or replace diseased or damaged tissue. To promote the formation of well-organized, functional tissue, scaffolds should closely resemble the structural and chemical characteristics of the natural extra cellular matrix (ECM). Ideally, the mechanical properties of scaffolds would mimic native biomechanics and be able to withstand *in vivo* stresses. Scaffold mechanics are of great importance as they have been shown to influence cellular behavior and the manner in which external mechanical signals are transferred to the cell [41,106].

Control of scaffold stiffness is of particular concern as stiffness can alter a large number of cellular functions including cell-matrix adhesions [41,42], size of the focal adhesions [42], stiffness and tension within the cell [41], motility and cell alignment [43,44], differentiation [46-48], propagation [45], viability [48], resistance to apoptosis [50] and phenotype [47,49]. For example, the addition of stiff microstructures within a soft gel regulated human mesenchymal stem cell (hMSC) proliferation and osteogenic gene expression [49]. hMSCs migrated preferentially to stiff microstructural elements within a three dimensional matrigel [49]. Similarly, osteogenic gene expression was reduced due to the increased stiffness of the gel scaffold [49]. Mouse myoblast cells,

cultured on patterned arrays of poly(dimethylsiloxane) (PDMS) columns covered with a thin layer of PDMS, tended to have high motility on softer regions of the PDMS substrate and preferentially migrated towards regions of higher stiffness [43]. NIH 3T3 fibroblasts have also been shown to migrate preferentially toward stiffer regions on collagen-coated polyacrylamide substrates [44]. These studies and many others support the hypothesis that cells sense their mechanical environment and alter their behavior in response to local changes in matrix stiffness.

Scaffold stiffness can be modulated by a wide array of methods including chemical crosslinking [44,107-109], varying hydrogel density [46], applying a bioactive coating to stiff bulk materials [42,44], and changing scaffold composition [47,48,78,110]. The ratio of poly-lactic acid (PLLA) to poly-lactic co glycolic acid (PLGA) can be varied to alter substrate stiffness and was utilized to study myoblast behavior on substrates of varying stiffness [48]. Hydrogel stiffness has also been controlled by varying the quantity of crosslinking agents used in the scaffold [46]. These approaches provide useful information about a cell's response to substrate stiffness but either lack consistency in chemistry [49], scaffold morphology [46] or the ability to assess cell growth within a three-dimensional scaffold [42,43,49]. Ideally, stiffness could be controlled within a 3D scaffold with no change in surface chemistry, bulk chemistry or scaffold architecture. A novel approach to control scaffold stiffness is to utilize coaxial electrospinning. The structure of the core material could be used to control the stiffness of the scaffold while presenting the cell with identical scaffold architectures and surface chemistries. This

method would perceivably provide a wide array of scaffold moduli without altering scaffold surface chemistry, scaffold density or adding costly processing steps such as functionalizing the surface of the fibers.

The goal of this study was to determine if feed rate [111], solution concentration [111-114], and solvent [112] could be used to control the core diameter of coaxial electrospun scaffolds as these parameters have previously been shown to influence single fiber properties. Subsequently, the influence of core diameter on scaffold mechanics was investigated in a PCL-gelatin core-shell model and compared to monofiber scaffolds and a 1:1 polymer blend.

3.2 Materials and Methods

3.2.1 Electrospinning

Eight different scaffolds were prepared including five coaxial scaffolds with the label CoA1 - 5 and a PCL, gelatin (Gel), and a 1:1 PCL-gelatin blend (Blend) sample. Coaxial electrospinning solutions were prepared by mixing a solution of gelatin (Sigma-Aldrich; St. Louis, MO) with 1,1,1,3,3,3-hexafluoro-2-propanol (HFP; Sigma-Aldrich Co., St. Louis, MO) at a concentration of 12 wt./vol.% and a solution of poly ε-caprolactone (PCL; Sigma-Aldrich; St. Louis, MO; M_n = 42,500) in HFP at varying concentrations. To fabricate control scaffolds, PCL, gelatin, and a blend of PCL and gelatin (1:1 mass ratio) were stirred in HFP at concentrations of 14, 12, and 12 wt./vol.% respectively.

All scaffolds were vertically electrospun onto an 8.5 cm^2 grounded plate at a distance of 20 cm. PCL, gelatin, and blend scaffolds were electrospun at a potential of 19-26kV with flow rates between 12-15 ml/hr. To manufacture the coaxial nanofiber scaffolds a coaxial nozzle consisting of a hollow stainless steel t-junction with a fully penetrating core needle was used to separate the core and shell solutions (Figure 3.1). Coaxial core concentrations and flow rate were altered to generate different core diameters (Table 3.1) with all coaxial scaffolds using a shell of 12 wt./vol.% gelatin at a rate of 4ml/hr. Acetone replaced 10 vol.% of the HFP in the core solution of sample CoA1. Coaxial scaffolds were electrospun at a potential of 15-18kV. All as-spun scaffolds were placed in a vacuum sealed desiccator until further use. Gelatin containing scaffolds were crosslinked in a 50mM solution of ethanol and N-(3-dimethylaminopropyl)-N'-ethylcarbodiimide hydrochloride (EDC; Sigma-Aldrich Co.) in pure ethanol for 24 hours prior to hydration.

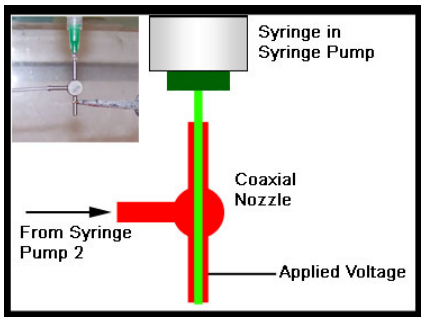

Figure 3.1. Coaxial electrospinning schematic.

Table 3.1. Electrospinning parameters for the coaxial PCL-gelatin fibers. All coaxial samples were spun with a shell solution of 12 wt./vol.% gelatin at 4ml/hr.

Scaffold Name	**Core Solution Concentration (wt./vol.%)**	**Core Solution Rate (ml/hr)**
CoA1	12	1
CoA2	8	1
CoA3	12	1
CoA4	10	2
CoA5	12	2

3.2.2 Scanning Electron Microscopy

Fiber morphology of the electrospun scaffolds was examined by scanning electron microscopy (FEI Sirion). Dry scaffolds were sampled by removing a punch biopsy from the as spun scaffold and were sputter coated with gold-palladium followed by imaging in secondary electron mode at 5 kV. Images were collected from each sample to characterize the overall fiber morphology. Dry fiber diameter was determined by measuring at least 100 fibers per sample at three different time points using Image J software. Since electrospun scaffolds do not have porosity, the distance between adjacent fibers in the same plane of the scaffolds were measured to quantify the free spaces in the scaffold. Inter-fiber distance was quantified by taking 15 measurements per scaffold in 2 different locations within the scaffold and 3 different scaffolds for a total of at least 90 measurements per condition. Measurements were reported as mean ± standard deviation.

3.2.3 Transmission Electron Microscopy

Fiber cross-sections from the coaxial samples were imaged using transmission electron microscopy (TEM) to characterize the core/shell morphology. As-spun scaffolds were crosslinked as described above; rinsed 2 X with Milli-Q water for 1 hour per rinse, and dried using lyophilization. Then the scaffolds were trimmed, mounted in epoxy, and sectioned on a Leica EM UC6 ultramicrotome cutting at 100 nm. Sections were examined with a FEI Tecnai G2 Spirit TEM operated at 100 kV.

3.2.4 Laser Scanning Confocal Microscopy

To assess any changes in core/shell morphology as a result of hydration, the coaxial electrospun scaffolds were imaged while hydrated using laser scanning confocal microscopy (Zeiss LSM 510 META). Prior to electrospinning, fluorescein (Fluka; Milwaukee, WI) and rhodamine B (Fluka; Milwaukee, WI) were loaded into the core and shell respectively at a concentration of 1 wt./vol.%. The diameter of the core was measured (n = 15 measurements) using the Zeiss LSM Image Browser software. Total fiber diameter was determined by measuring 100 fibers per sample using Image J software. Measurements were reported as mean ± standard deviation.

3.2.5 Tensile Testing

Ultimate tensile strength (UTS), linear stiffness, and elongation at failure were quantified using uniaxial tensile testing. Each scaffold (n = 6 per group) was crosslinked, hydrated using HEPES buffered saline (HBS), and punched into dog-bone shaped tensile specimens with a width of 4 mm and gauge length of 20 mm. The samples were secured in the grips of a tensile tester (TestResources 100R; Shakopee, MN) and loaded until

failure at a rate of 2 mm/sec to prevent scaffold dehydration. Mechanical properties were reported as mean ± standard deviation.

3.2.6 Statistical Analyses

All data was analyzed using SigmaStat 3.10 (Systat Software Inc; San Jose CA). Correlations were determined using the Pearson's correlation coefficient. Differences between the experimental and control groups were analyzed using Student's t-tests. P values equal to or less than 0.05 were considered statistically significant.

3.3 Results

Control and coaxial electrospun materials, fabricated under all conditions, exhibited random fiber orientation (Figure 3.2). Dry, as-spun fibers were round in cross-section for the PCL, PCL-Gel blend and the CoA1, CoA3, CoA4, and CoA5 conditions whereas the pure gelatin and CoA2 fibers possessed a distinct ribbon-like morphology (Figure 3.2). No significant difference in fiber diameter was found between the as-spun coaxial scaffolds which ranged in diameter from 2.6-3.6 μm at the minimum and maximum. The blend and PCL were thinner than all other scaffolds and were measured to be 0.95 ± 0.32 μm and 0.63 ± 0.25 μm in diameter respectively. Interfiber distance measurements (Figure 3.4) of the gelatin versus the coaxial scaffolds were not significantly different and were measured at 17.85 ± 6.95 μm in the gelatin scaffold and ranged from 15.1-22.4 μm in the coaxial scaffolds. The interfiber distances of the blend

and PCL were smaller than most other scaffolds and were measured to be 6.56 ± 2.7 µm and 4.54 ± 1.81 µm respectively.

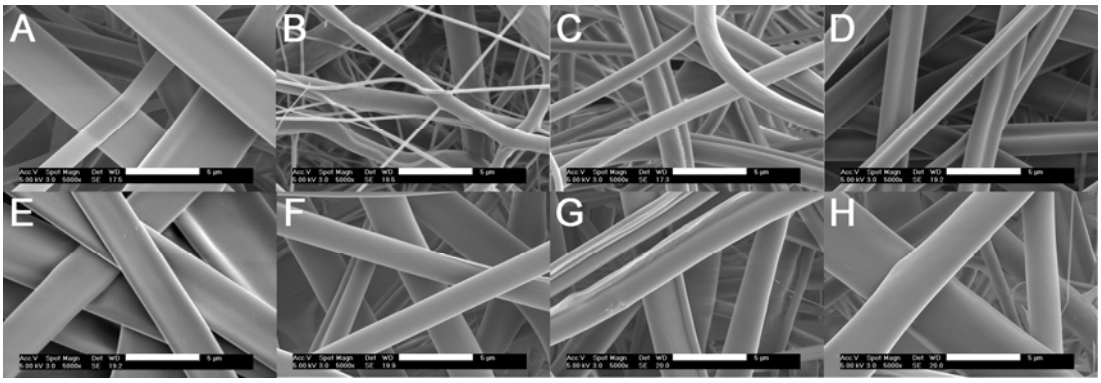

Figure 3.2. Scanning electron micrographs of as-electrospun scaffolds. As-spun A) gelatin, B) PCL, C) Blend, D) CoA1, E) CoA2, F) CoA3, G) CoA4 and D) CoA5. Scale bar = 5µm.

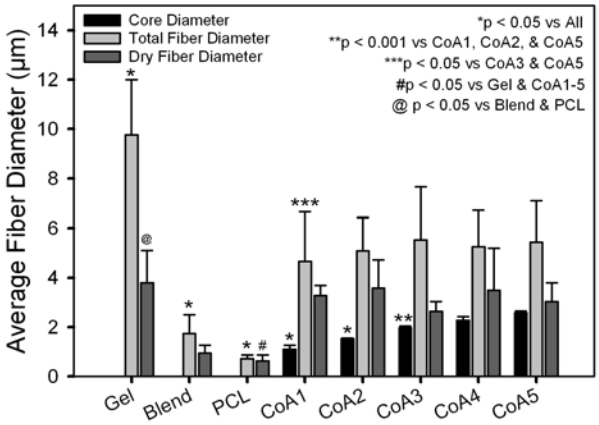

Figure 3.3. Fiber diameter of hydrated electrospun scaffolds.

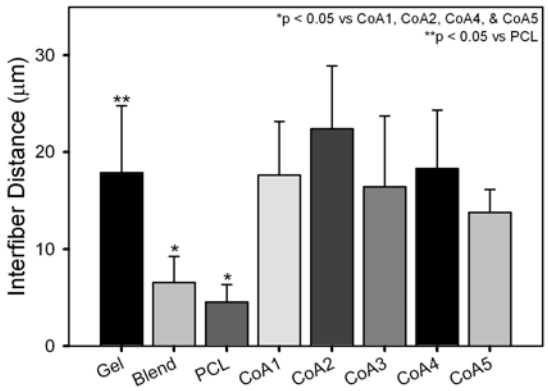

Figure 3.4. Interfiber distance of as-electrospun fibers.

As these scaffolds are intended to be utilized in their hydrated form, all subsequent analysis was performed on hydrated scaffolds. Fiber structure was visualized through fluorescent dye additions to the individual polymer components. Confocal microscopy revealed that pure gelatin scaffolds swelled once hydrated with gelatin fibers increasing in width to 9.76 ± 2.24 μm (Figure 3.3 and Figure 3.5). The PCL fibers were significantly smaller than all other fibers at 0.72 ± 0.14 μm and the blend fibers were measured at 1.74 ± 0.77 μm. PCL and PCL-gelatin blend scaffolds were comprised of thinner fibers with the PCL and gelatin undergoing slight polymer segregation in the blend as seen by the domains of pure PCL and pure gelatin within each fiber (Figure 3.5C). Coaxial morphology, defined as fibers consisting of a red shell and green core, was seen in greater than 81-92% of all fibers in the double nozzle electrospun scaffolds (Figure 3.5D-H). Fibers in the coaxial groups which did not exhibit the core-shell morphology were significantly smaller in diameter.

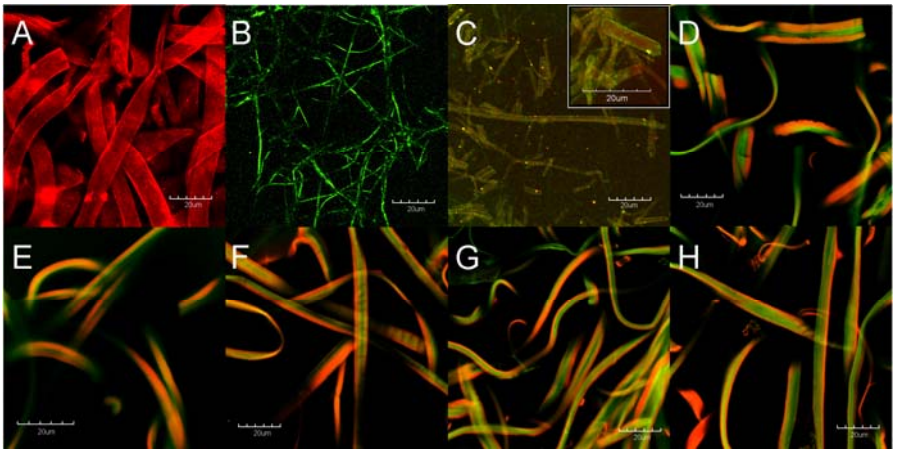

Figure 3.5. Laser scanning confocal micrographs of hydrated coaxial scaffolds A) Gelatin, B) PCL, C) Blend, D) CoA1, E) CoA2, F) CoA3, G) CoA4, and H) CoA5. Scale bar = 20μm.

Increases in both the core solution concentration and flow rate generated coaxial fibers with the largest core diameter (2.58 ± 0.07 μm) while lower solution concentrations and low feed rates resulted in thin cores (from 1.10 ± 0.17 μm) (Table 3.1 & Figure 3.3). One anomaly to the trend was seen with a core solution with 12 wt./vol.% PCL in a solution of acetone and HFP (1:9 volume ratio). Despite having a relatively high solution concentration, this solution (CoA1) produced the thinnest core when spun at 1ml/hr. While the core diameter increased with concentration and flow rate, the measurements of the total fiber diameter showed no explicit trend.

To further characterize the coaxial scaffold morphology, TEM analysis was performed on cross-sections of the coaxial fibers. As expected the core/shell morphology was seen for all coaxial electrospun samples in a majority of all fibers observed (Figure

3.6). Fibers without coaxial morphology had significantly smaller diameters. This analysis also revealed slight variations in fiber morphology that may have influenced the final properties. Ribbon like fibers were very predominant in the CoA2 fibers (Figure 3.6B) and the cores, though thin, expanded to a significant portion of the fiber width. Similar to the CoA2 fibers, CoA3 fibers had a more ribbon-like appearance than other coaxial fibers (Figure 3.6C) however the total width of the fibers was smaller than in CoA2 (Figure 3.3) and rounded fibers were also observed. The CoA1 fibers were characteristically small and maintained a rounded appearance with well contained round cores (Figure 3.6A). CoA4 scaffolds appeared to have irregular core morphology where cores were rounded in shape but possessed lobes (Figure 3.6D). The CoA4 and CoA5 fibers were relatively similar in overall fiber shape with both scaffold cores fully sheathed by the gelatin shell.

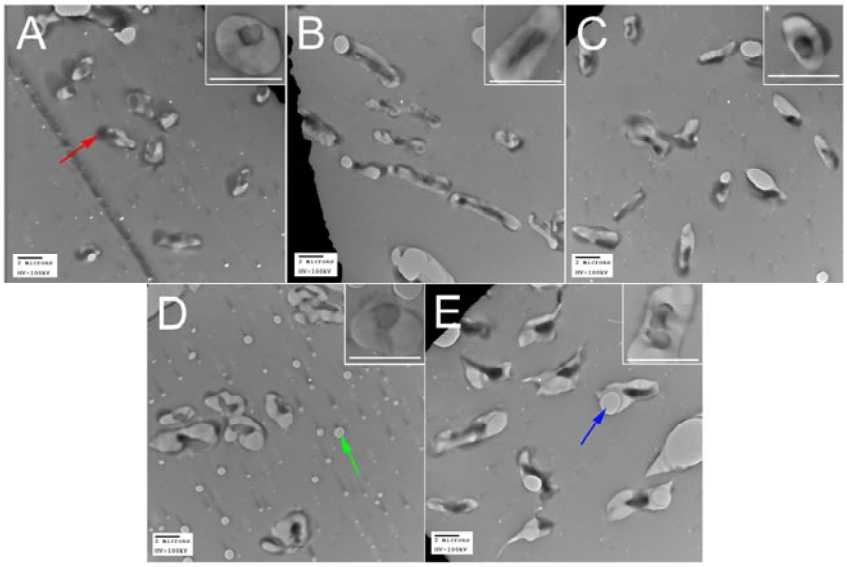

Figure 3.6. Transmission electron micrographs of previously hydrated coaxial electrospun scaffolds A) CoA1, B) CoA2, C) CoA3, D) CoA4, and E) CoA5. Insets are higher magnification images of the fibers. The arrows indicate defects in the micrographs created by the sample preparation process. The red arrow indicates a dark "shadow" near a coaxial fiber. The green arrow indicates a pore in the epoxy matrix. The blue arrow indicates a hole in the section that formed between the coaxial fiber and epoxy matrix. Scale bar = 2μm.

The mechanical properties of the individual scaffold components, PCL and gelatin, are drastically different. Stiffness values, calculated as the slope of the linear region in the stress strain curve, of the gelatin were 338.82 ± 67.01 kPa while the elastic modulus of the PCL was 12,198.44 ± 1,816.18 kPa (Figure 3.7A). The PCL and PCL-Gel blend were significantly stiffer than all other scaffolds. Core diameter was a significant determinant of scaffold stiffness with stiffness increasing from 402.94 ± 67.59 kPa to 1,613.82 ± 670.29 kPa in the CoA1 to the CoA5 scaffolds respectively (Figure 3.7A).

The core diameter positively correlated with stiffness ($r^2 = 0.85$, Figure 3.7B). The stiffness of the CoA1 scaffold and the gelatin scaffold were not significantly different, however all other coaxial scaffolds were significantly different than gelatin. With the addition of thin PCL cores to the gelatin fibers, the strength of the CoA1 scaffold significantly increased to 361.91 ± 114.76 kPa from the pure gelatin scaffold at 223.06 ± 43.58 kPa (Figure 3.7C). Coaxial scaffold strength significantly increased with increasing core diameter from 361.91 ± 114.76 to 623.17 ± 87.26 kPa in samples CoA1-CoA5. Fiber core diameter positively correlated with strength ($r^2 = 0.88$, Figure 3.7D); however only CoA1, CoA3, and CoA5 were statistically different (Figure 3.7C).

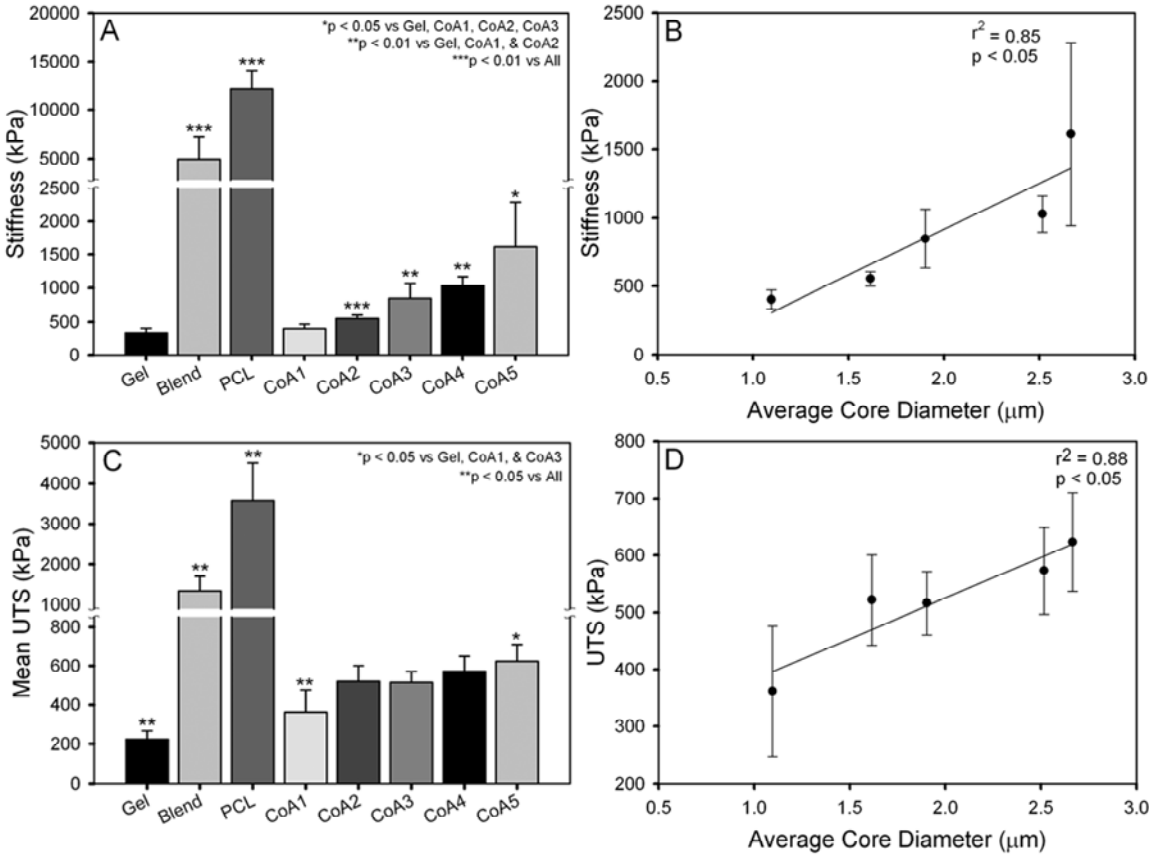

Figure 3.7. Stiffness of scaffolds (A), correlation of stiffness and fiber diameter (B), ultimate tensile strength (UTS) of scaffolds (C), and correlation of UTS with fiber diameter (D).

3.4 Discussion

Solvent, solution concentration, and feed rate have all been shown to influence the fiber diameter of electrospun scaffolds [111-114]. Applying these techniques to coaxial electrospinning was an easy method for controlling the core diameter in this study (Figure 3.3 and Figure 3.5). A decreased concentration and reduction in the core feed rate

decreased the core diameter. Reducing the PCL concentration was used to decrease the core diameter of the CoA3 scaffold when compared with the CoA2 scaffold. Reducing the core feed rate from 2mL/h to 1mL/h was used to decrease the core diameter observed in the CoA3 scaffold compared to sample CoA5. Acetone was added to the core solution of sample CoA1 prior to electrospinning in a successful attempt to decrease the core diameter. When the core diameter of sample CoA1 is compared with sample CoA3, which was spun under the same conditions without the acetone, the core diameter was significantly decreased in sample CoA1 (Figure 3.3). Different solvents have been utilized to modulate fiber diameter of the same material in previous studies [112,115,116] with lower viscosity solutions correlating to smaller fiber diameter.

The processing variables, solution concentration, solvent and feed rate, not only controlled core fiber diameter but also dictated core morphology (Figure 3.6). CoA2 exhibited ribbon-like fibers with thinner elongated cores. This type of fiber morphology was previously reported to be a result of rapid solvent evaporation, forming a skin, followed by collapse of this skin [117]. In a polymer solution with a low solids content such as the core solution of CoA2 (8 wt./vol.%), the solvent likely evaporates more rapidly due to the relatively high concentration of solvent to polymer leading to rapid polymer solidification on the outer surface followed by slow solidification in the center. This would be even more pronounced in the low humidity environment (~25% relative humidity) in which the scaffolds were electrospun.

Coaxial electrospinning parameters significantly controlled core diameter of the fibers with little effect on as-spun total fiber diameter and interfiber distance (Figure 3.3 and Figure 3.4). Based on these analyses the scaffold structure is very similar between the gelatin and coaxial scaffolds. As it is desired to alter only scaffold mechanics and not scaffold architecture, the coaxial scaffolds may provide a three dimensional growth template for study that lacks the complications seen with other stiffness model systems.

Based on the results of mechanical testing, the coaxial scaffolds were significantly stiffer than the gelatin scaffold but not as stiff as the PCL and blend scaffolds (Figure 3.7A). As the core diameter of the coaxial electrospun scaffolds increased the stiffness also increased (Figure 3.7B). PCL has a greater stiffness than gelatin and therefore the PCL will be the load bearing constituent of the scaffold. Based on this, small variations in the PCL core diameter or scaffold content will significantly alter the stiffness of the scaffold. Since both the PCL and blend scaffolds had greater PCL content than the coaxial scaffolds it is logical that the 100% PCL and the blend scaffolds has greater stiffness. An increase in electrospun scaffold strength and stiffness with increasing fiber diameter has been observed before [118]. Therefore the results of this study are consistent with previous studies and the expected trend was observed for the coaxial scaffolds.

As anticipated, the strength of the coaxial electrospun scaffolds increased with increasing core diameter (Figure 3.7C & D). Previous studies have reported increased strength and stiffness of hydrated PCL-core/gelatin-shell electrospun scaffolds over 100% gelatin scaffolds and a lower strength and stiffness when compared with 100%

PCL scaffolds [119]. Therefore the results demonstrated in this study are consistent with previous work; however variations in core diameter were not studied with respect to controlling the mechanical properties. The general trend observed for scaffold strength was an increase with increased core diameter. Some inconsistencies in this trend were observed for scaffolds CoA2-CoA4 and may be due to the lack of statistically significant differences in the measured core diameter of these scaffolds (Figure 3.7C). A possible source of inconsistencies in the mechanical property trend may be the variations in observed fiber geometry (Figure 3.6). As discussed previously the CoA2 scaffolds had a ribbon-like structure and the CoA4 scaffold had an irregular core shape. These two aspects may have influenced the interfacial strength or may directly influence the mechanical properties. For instance, mechanical interlocking between the core and shell may have increased the fiber strength.

3.5 Conclusions

The data indicates that coaxial electrospinning can be used to engineer the strength and stiffness of a tissue engineering scaffold. Core diameter can be varied by altering solution concentration, core feed rate, and solvent resulting in tailorable mechanical properties. This scaffold manufacturing method creates scaffolds with varying degrees of stiffness with little or no alterations in scaffold architecture or chemistry. As a result, these scaffolds could be utilized to assess cellular response to 3D

stiffness without confounding factors such as increased crosslinking density, changes in chemistry or time consuming surface modifications.

3.6 Acknowledgments

This study was funded in part by an instrumentation and facilities grant from the Institute for Materials Research (IMR) at The Ohio State University. I would also like to thank the Campus Microscopy and Imaging Facility at OSU for the use of the confocal microscope and transmission electron microscope and the Campus Electron Optics Facility for the use of the scanning electron microscope.

Chapter 4: Engineered Skin Biomechanics: Enhanced Tissue Strength via Coaxial Fiber Scaffolds

4.1 Introduction

Within the U.S., 2.4 million burn injuries are reported annually [120] with an estimated 4,500 mortalities [121]. During times of military conflict, the number of burn injuries dramatically increases burns account for 5-20% of military casualties [122]. Advances in burn care, such as improved infection control [123-125], have decreased mortality rates [126] making wound management even more critical. Split-thickness autograft (AG) is the standard wound treatment for full-thickness burns. In large burns sparse availability of uninjured skin prevents rapid closure of the wound resulting in increased scar tissue formation (Figure 1.1) or mortality.

As a result of this, alternate wound closure strategies have been investigated. Tissue engineered skin offers promise when autografts are not available; numerous tissue engineered skin replacements have been created [127-133]. Engineered skin cannot restore all functions of normal human skin. However, it has been shown to reduce: 1) donor site area required to permanently close wounds, 2) mortality, and 3) morbidity from scarring [8,134,135]. Unfortunately, engineered skin is orders of magnitude weaker than normal human skin, difficult to surgically apply, subject to damage by mechanical shear and exhibits significantly less elasticity, altering mobility [54]. While the potential clinical impacts of engineered skin are substantial, if mechanical function is to

approximate normal human skin major advances in our scientific knowledge of how such complex cellular communities can be controlled is required. New innovations in engineered skin design and culture are needed. Increasing the strength of engineered skin is one area that can be significantly improved through the development of materials technology.

Increasing the strength of engineered tissue is generally achieved by the use of scaffold crosslinking [23,34,39,57-65,69], protein-synthetic blends [12,38,58,69], and synthetic polymer scaffolds [79]. In every case reduced cellular or tissue viability has been observed either at elevated concentrations of crosslinker [23] or due to PCL-cell interactions [12]. These approaches are not ideal due to the reduced cell viability observed in every case. An alternative approach is to add PCL as a core to electrospun protein fibers. Coaxial electrospinning has been used to add a synthetic core to a gelatin fiber, increasing the strength of the scaffold while maintaining a continuous biologically active shell. By adding PCL to the core of the fibers the strength is increased and the influence of coaxial scaffolds on tissue growth can be studied.

The goal of this study was to determine if coaxial electrospun scaffolds with increasing strength and stiffness could be utilized to engineer human skin with mechanical properties that scaled proportionally with the scaffold properties. Control of scaffold mechanics was achieved by modifying core-shell fiber core diameter as previously described (Chapter 3). The effect of core diameter on both scaffold and

engineered skin (ES) mechanical properties and ES morphogenesis was investigated and compared with electrospun gelatin, PCL and gelatin-PCL blended scaffolds.

4.2 Materials and Methods

4.2.1 Scaffold Fabrication

Electrospinning solutions were made as described previously (Chapter 3). Briefly, gelatin (Sigma-Aldrich; St. Louis, MO) or polycaprolactone (PCL; Sigma-Aldrich; St. Louis, MO; M_n = 42,500) were dissolved in 1,1,1,3,3,3-hexafluoro-2-propanol (HFP; Sigma-Aldrich; St. Louis, MO) at different concentrations. A total of seven scaffolds were made including four coaxial and three control samples. The coaxial scaffolds were all spun with a 12 wt/vol. % solution of gelatin in HFP for the shell of the fiber and the PCL core concentrations were varied from 8-12 w/v %. The core concentrations were specifically 12, 8, 12, 10, 12 wt./vol.% for samples CoA1, CoA2, CoA3, CoA4, and CoA5 respectively (Table 4.1).

Table 4.1. Concentrations of coaxial electrospinning solutions.

Scaffold Name	**Core Solution Concentration (wt./vol.%)**	**Core Solution Feed Rate (ml/h)**
CoA1	12 with 10% acetone	1
CoA2	8	1
CoA3	12	1
CoA4	10	2
CoA5	12	2

Acetone replaced 10 vol.% of the HFP in the core solution of sample CoA1 so the ratio of HFP:Acetone was 9:1. The three control solutions were PCL, gelatin (Gel), and a blend of the two (Blend) and were electrospun at 14, 12, and 12 w/v % in HFP respectively. The Blend was a 1:1 mixture of gelatin and PCL by volume.

PCL, Gel, and Blend control scaffolds were electrospun at flow rates of 15, 12 and 12 ml/hr respectively at a voltage of 26kV, 23kV, and 19kV respectively onto an 8.5 cm^2 grounded plate at a distance of 20 cm. Coaxial scaffolds were electrospun at a potential of 15-20kV. The flow rate of the gelatin shell was at 4ml/h for all samples and the core was at 1 ml/hr for samples CoA1, CoA2, and CoA3 and 2 ml/hr for samples CoA4 and CoA5. After electrospinning the samples were stored in a vacuum sealed desiccator. Prior to use all scaffolds containing gelatin were crosslinked in a 7mM solution of ethanol and N-(3-dimethylaminopropyl)-N'-ethylcarbodiimide hydrochloride (EDC; Sigma-Aldrich Co.).

4.2.2 Formation of Engineered Skin

Crosslinked scaffolds were seeded with human primary dermal fibroblasts (HF) at a density of 0.5 x 10^6 cells/cm^2 and epidermal keratinocytes (HK) at a density of 1.0 x 10^6 cells/cm^2. Both HF and HK were obtained by isolating cells from surgical discard tissue with approval from the Institutional Review Board at the Ohio State University. After inoculation of HF, the material was incubated at 37^{o}C and 5% CO_2 in UCMC 160

medium for 1 day followed by inoculation of HK. 1 day after inoculation of HK the tissue was placed on a perforated stainless steel frame with a cotton sheet in between the frame and tissue. The tissue was then cultured for 21 days at the air-liquid interface.

4.2.3 Tensile Testing

Tensile testing was used to quantify the mechanical properties of acellular scaffolds and engineered skin (n = 6 for each condition). Acellular scaffolds were prepared for mechanical testing by crosslinking each scaffold in a 7mM solution of N-(3-dimethylaminopropyl)-N'-ethylcarbodiimide hydrochloride (EDC; Sigma-Aldrich Co.) and 100mL of pure ethanol for 24 hours, hydrated using HEPES buffered saline (HBS), and punched into dog-bone shaped tensile specimens with a width of 4 mm and gauge length of 20 mm. Engineered skin was cultured for 19 days prior to tensile testing. The samples were secured in the grips of a tensile tester (TestResources 100R; Shakopee, MN) and loaded until failure at a rate of 2 mm/sec to prevent scaffold dehydration. Data from samples which did not break within the gauge length were discarded. Ultimate tensile strength (UTS) and stiffness were measured and reported as mean ± standard deviation.

4.2.4 Surface Electrical Capacitance

Surface electrical capacitance (SEC) was performed to quantify the surface hydration of the engineered skin. Surface hydration has been previously reported to be an accurate, reproducible method to non-destructively assess barrier function in skin where barrier function is inversely proportional to SEC. On culture days 7, 13, and 19, SEC

measurements (n=6 per scaffold) were collected from the engineered skin using a NOVA dermal phase meter (DPM 9003; NOVA Technology; Portsmouth, NH). Results are expressed as surface electrical capacitance ± standard deviation.

4.2.5 Immunohistochemistry

Biopsies were taken from the engineered skin for histology at day 19. The biopsies were embedded in OCT resin and stored at -80^{o}C until sectioning. For immunostaining, slides were fixed in methanol for 8 min, rehydrated in PBS and incubated in primary antibodies for human involucrin (Molecular Probes; Eugene, OR), human collagen type IV (Molecular Probes; Eugene, OR) at 4C overnight. The following day the sections were stained with the appropriate secondary antibody along with DAPI for 1 hour at room temperature. Sections were rinsed with PBS, mounted with glycerin and cover-slipped. The stained sections were imaged using an Olympus FV1000 Multi-Photon confocal microscope.

4.2.6 Cellular Metabolism

A modified MTT assay was performed to quantify the cellular metabolic activity within the engineered skin. At culture days 7, 13, and 19, 4 mm punch biopsies were removed (n = 6 per group, n = 6 per time point) and immediately assessed following a protocol previously described [40]. Briefly, 0.5 ml of a sterile-filtered solution of 0.5 mg MTT/ml PBS was added to each well of a 24-well plate, containing one 4 mm punch. The biopsies were incubated in the MTT solution for 3 hours at 37ºC and 5% CO_2. After three hours, the MTT solution was aspirated from the well, 0.5 ml methoxyethanol was added

to each well (Fisher Scientific; Fair Lawn, NJ), and the solution was agitated on a rocking plate for 3 hours to dissolve the formazan crystals. The amount of MTT-formazan product released was measured at 590 nm on a microplate reader with values reported as mean optical density ± standard deviation.

4.2.7 Statistical Analysis

All data was analyzed using SigmaPlot 3.10 (Systat Software Inc; San Jose CA). Differences between the groups were analyzed using Student's t-tests. P values less than 0.05 were considered statistically significant.

4.3 Results

4.3.1 Mechanical Properties of Acellular Scaffolds

Core diameter in this study was controlled using the same method as described previously (Chapter 3). These methods include varying the core feed rate, core solution concentration, and changing the solvent used to dissolve the PCL (Table 4.1). Ideally, a tissue engineering scaffold would provide a highly bioactive surface for cell adhesion and migration and also provide high strength to withstand *in vivo* stresses and for better handling during surgical implantation. The addition of PCL in the core of the gelatin fiber provides strength while maintaining the bioactivity of the scaffold. With even a thin PCL core within the gelatin fibers, the strength of the scaffold was significantly increased (Figure 4.1A) from 105.90 ± 25.52 kPa in the pure gelatin to 334.90 ± 90.85 kPa in the

CoA1 scaffold. The strength of the coaxial electrospun scaffolds was dependent on the size of the PCL core. With an increase in core diameter the strength and stiffness also increased. The strength of the coaxial scaffolds increased from 334.90 ± 90.85 to 711.30 ± 115.48 kPa from the CoA1 to the CoA5 samples respectively. Scaffold CoA2 was not significantly different than CoA1 or CoA3 in strength or stiffness so the scaffold was not used to form engineered tissue. The strength of the Blend scaffold was not significantly different than CoA4 or CoA5 while the strength of the PCL was significantly higher than all other scaffolds at 3582.97 ± 931.31 kPa.

A similar trend was seen in the stiffness of the coaxial samples (Figure 4.1B). Increasing the PCL core diameter increased the stiffness of the coaxial scaffolds from 991.23 ± 271.67 kPa to 2942.72 ± 276.59 kPa in the CoA1 to the CoA5 scaffolds respectively. PCL was measured to have a significantly higher stiffness than all other samples at 12198.44 ± 1816.18 kPa, the blend had a stiffness of 2397.95 ± 1339.30 kPa, and the gelatin had a significantly lower stiffness of 164.71 ± 26.23 kPa. The stiffness of the gelatin scaffold was significantly lower than all other samples.

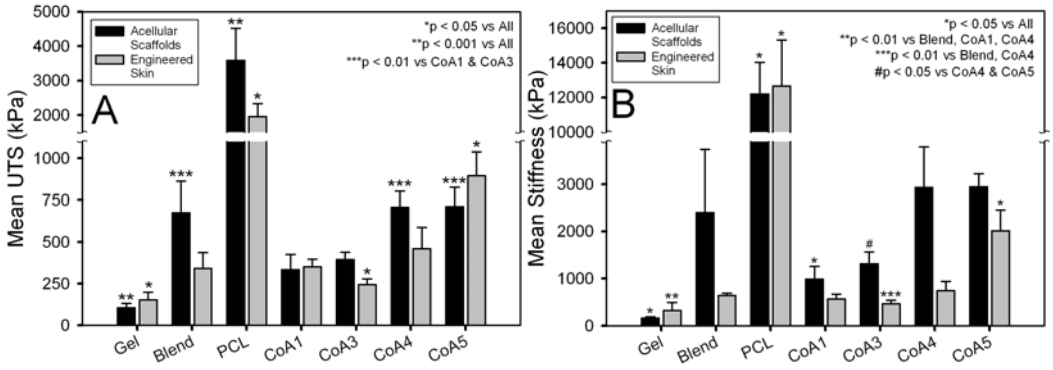

Figure 4.1. Mechanical properties of hydrated acellular scaffolds and engineered skin. Scaffolds include gelatin, PCL, gelatin-PCL blend, and gelatin-shell/PCL-core coaxial scaffolds. Mean ultimate tensile strength (A) and mean stiffness (B).

4.3.2 Mechanical Properties of Engineered Skin

The engineered skin cultured on the coaxial scaffolds was significantly stronger than the tissue formed on the gelatin scaffold excluding sample CoA3 (Figure 4.1A). The strength of the tissue cultured on the gelatin was 153.46 ± 45.69 kPa which was not as strong as the blend and PCL at 341.06 ± 95.52 kPa and 1953.67 ± 376.50 kPa respectively. PCL was significantly stronger than all other scaffolds. The skin formed on the coaxial scaffolds increased in strength from CoA1 at 352.11 ± 44.39 kPa to CoA5 at 894.81 ± 143.95 kPa. Engineered skin formed on sample CoA3 was higher in strength than gelatin but had significantly lower strength than all other scaffolds. CoA1 and CoA4 were not significantly different while CoA5 was significantly stronger than all the coaxial skin.

Tensile testing of the engineered skin showed very few improvements in the mechanical properties of the tissue (cells and scaffold) after 19 days in culture compared to the acellular scaffolds (Figure 4.1A). The strength of the engineered skin was lower than that of the acellular scaffold in the Blend, PCL, CoA3, and CoA4 group. There were two groups in which an increase in strength was observed, gelatin and CoA5. The gelatin scaffold had an increase in strength from 105.90 ± 25.52 kPa to 153.46 ± 45.69 kPa. Similarly sample CoA5 had an increase in strength from 711.30 ± 115.48 kPa to 894.81 ± 143.95 kPa after culture of engineered skin. No change in strength was observed for scaffold CoA1.

Stiffness values of the scaffolds decreased in the engineered skin versus the acelluar scaffold for all groups excluding gelatin and PCL (Figure 4.1B). No change in stiffness was observed in the PCL stiffness. No difference in elongation at failure between the acellular scaffolds and engineered skin was observed with the exception of PCL which experienced a large decrease in elongation at failure after 19 days of culture.

4.3.3 Viability and Organization of Engineered Skin

Cell viability was quantified using an MTT assay and the results showed lower average cellular metabolism in the PCL scaffold than all other scaffolds at all time points (Figure 4.2). At day 7 the blend and PCL scaffolds were not significantly different although the PCL had much lower cellular activity than every other scaffold. At day 19 the gelatin scaffold showed a greater metabolic activity than the blend, PCL, and CoA5 sample.

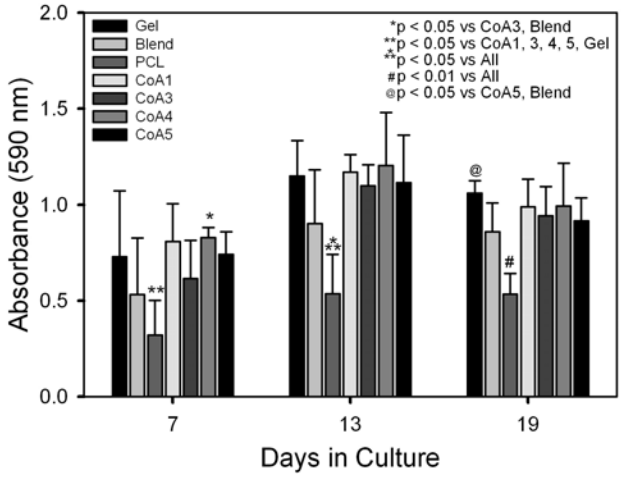

Figure 4.2. Metabolic activity assay (MTT) of the engineered skin cultured on respective scaffolds for 7, 13, and 19 days in culture.

To assess epidermal differentiation and barrier formation, surface hydration was measured using electrical capacitance (SEC). At culture day 7, the engineered skin was moist with little difference between groups (Figure 4.3). By day 13, no statistically significant differences between the engineered skin grown on coaxial and gelatin scaffolds was observed. However, engineered skin made with pure gelatin scaffolds had reached normal human skin values and was significantly lower than the CoA1, 4, and 5 coaxial scaffolds at day 19 (Figure 4.3). The engineered skin grown on CoA3, blend, and PCL scaffolds had higher SEC measurements throughout the culture period.

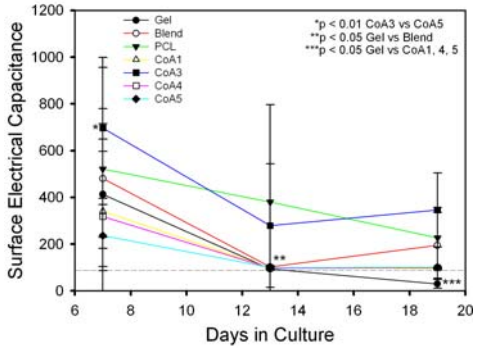

Figure 4.3. Surface electrical capacitance of engineered skin measured at 7, 13, and 19 days in culture. Dashed line represents surface electrical capacitance of normal human skin.

Immunostaining revealed engineered skin formed using coaxial electrospun scaffolds were well populated by fibroblasts (Figure 4.4D-G). Similarly the gelatin and Blend groups supported high densities of fibroblasts within the scaffold (Figure 4.4A&B). In contrast, fibroblasts within the PCL were sparse (Figure 4.4C). Stratification of the dermal and epidermal layers was observed in the gelatin, blend, and CoA4 scaffolds (Figure 4.4A&F). Epidermal and dermal layers appeared to be intermixing in all other scaffolds with a poorly defined dermal-epidermal junction (Figure 4.4C-E&G). The basal layer of epidermal keratinocytes which is responsible for maintaining the epidermis is not present in engineered skin from the PCL, CoA1, CoA3, and CoA5 scaffolds (Figure 4.4C-E&G). Basement membrane formation, as evidenced by a thick, continuous layer of collagen type IV, was observed in gelatin, Blend, CoA1, CoA3, and CoA4 groups (Figure 4.4A,B&D-F). Diffuse, non-continuous staining for collagen type IV was

observed in engineered skin from the PCL and CoA5 groups. Positive staining for involucrin, a suprabasal marker of epidermal differentiation, was observed in all samples; however in the PCL, CoA1, and CoA5 groups, staining was very sparse.

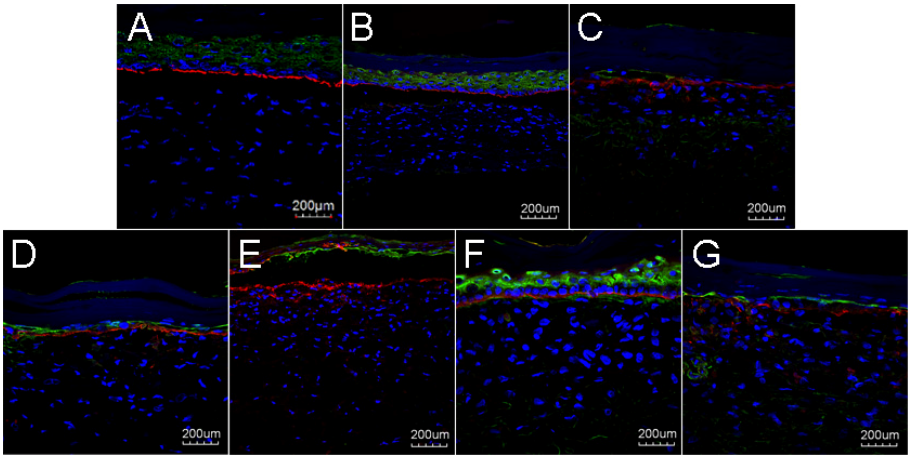

Figure 4.4. Engineered skin fabricated using A) pure gelatin, B) gel-PCL blend, C) pure PCL, D) CoA1, E) CoA3, F) CoA4 and G) CoA 5 scaffolds. Sections were immunostained for human involucrin (green), human collagen type IV (red), and DAPI (blue).

4.4 Discussion

The strength of engineered skin is important to prevent graft failure *in vivo* and *in vitro*. As engineered skin matures, the dermal fibroblasts will deposit extracellular matrix (ECM) components to replace the temporary scaffold. Sufficient time is required for deposition of the ECM and during this time the scaffold must support the structural

demands of the tissue. Commonly, engineered skin is formed using pure protein scaffolds and as a result the scaffolds are weak and susceptible to damage during the grafting procedure and during engraftment.

Combinations of bioactive proteins and synthetic polymers have been investigated as a potential solution to this problem. One common method is to use an electrospun blend of the two different materials [12,83,136]. Although the strength was increased with increased PCL content, the ability of these scaffolds to promote the formation of engineered skin was reduced when compared with a 100% collagen scaffold [12]. This was believed to be due to domains of PCL formed within individual fibers and the interaction of cells with these PCL domains [12]. The advantage of coaxial electrospinning over this method is that each fiber is coated with a bioactive gelatin shell limiting the exposure of cells to the PCL reinforcement. Other studies already demonstrated the ability coaxial electrospun scaffolds have of supporting cellular adhesion and proliferation. These studies found the coaxial scaffolds to be improved when compared with a 100% synthetic polymer scaffold [137,138], better than a collagen coated PCL scaffold [38], and not significantly different than a 100% collagen scaffold [38].

In a scaffold made of PCL-core/gelatin-shell nanofibers, the initial scaffold strength would be greater than 100% gelatin and the PCL fibers would remain within the tissue to provide strength long after the gelatin is degraded. In this study the ultimate tensile strength of the coaxial scaffolds was greater than the 100% protein scaffold

strength (Figure 4.1). This result was similar to the previous study of the influence of core diameter on scaffold mechanical strength (Chapter 3). The samples with a larger core diameter, specifically samples CoA4 and CoA5, had significantly higher strength and stiffness than samples CoA1 and CoA3 which both had smaller core diameters (Figure 3.1). Scaffold CoA2 from the previous study was not used to form engineered skin in this study since the strength of the scaffold was not significantly different than the strength of CoA1 or CoA3 (Chapter 3).

The formation of a well developed skin graft with high strength was the ultimate goal of this study. Growth of skin on gelatin was the standard to improve upon since skin cells have been shown to grow best on a 100% protein scaffold when compared with synthetic scaffolds [12,139]. Skin grown on all coaxial scaffolds was significantly stronger than the skin grown on gelatin alone (Figure 4.1A). Similarly the strength of the blend and PCL scaffolds with skin were also significantly stronger than the tissue grown on the gelatin scaffold. The increased strengths observed are likely due to the PCL reinforcement that remained in the scaffold after tissue culture, combined with the formation of dermal and epidermal constituents within the scaffolds. Growth of tissue within tissue engineering scaffolds has been shown to significantly improve the mechanical properties of the scaffolds [12,23]. The strength of the engineered tissue formed on the gelatin scaffold increased the strength of the acellular scaffold though it was not as strong as the skin formed on any other scaffold. The strength of both the gelatin and CoA5 scaffolds increased with engineered tissue formation while CoA1 did

not change and all other scaffolds had a decrease in strength. This trend is opposite of what was observed in previous studies [12,23] and is believed to be due to poorly developed tissue. Since the coaxial engineered skin mechanical strength was greater than the tissue formed on the gelatin, it is believed that the scaffold supported the majority of the load not the tissue that was grown on the scaffold. Therefore scaffold strength regulated engineered skin strength in this case.

Each scaffold was capable of promoting cellular attachment and growth; however, the MTT assay revealed a significantly lower cellular activity in the PCL scaffold at all time points (Figure 4.2). The other scaffolds were not significantly different than one another although ES fabricated with the PCL-gelatin blend scaffold exhibited lower average cellular metabolism compared to the gelatin and coaxial groups at each time point (Figure 4.2). A lower cellular affinity has been previously reported on synthetic scaffolds when compared with natural polymer scaffolds and a lower cellular affinity has been reported on synthetic/natural polymer blends when compared with a 100% natural polymer scaffold [12]. After 19 days in culture, the CoA5 group had lower cellular metabolism than the gel scaffold (Figure 4.2) likely due to the increased quantity of PCL within the scaffold. Although the core has been shown to be well contained within the shell, a small percentage of the observed fibers were not coaxial and were likely comprised of PCL given their size (Chapter 3). As the concentration of PCL in the scaffold is increased, the interactions of cells with PCL would have also increased and therefore a decreased cellular activity would be observed. Despite the decreased cellular

activity on the CoA5 scaffold versus the gelatin scaffold, the remaining coaxial scaffolds were not significantly different than gelatin at any other time point, excluding day 7 where scaffold CoA4 had a higher cellular activity than the gelatin scaffold (Figure 4.2). Since the cellular activity of the coaxial scaffolds was very similar to gelatin, while the blend and PCL showed reduced cellular activity at each time point it is believed that the majority of cell-scaffold interactions in the coaxial scaffolds were between the cells and the protein shell.

SEC of healthy human skin should have a surface electrical capacitance close to the dashed line indicated in Figure 4.3 [140]. In this study, the SEC values of engineered skin were very close to this value by day 13; only samples CoA3 and PCL were considerably larger. By day 19 the Gel, CoA1, CoA4 and CoA5 scaffolds were close to the value of normal human skin. At day 19 the blend, PCL and CoA3 had SEC values that were considerably higher than normal human skin. The increase in SEC values observed in both the CoA3 and Blend samples from day 13 to day 19 has been observed in similar studies of the surface electrical capacitance of engineered skin and has been attributed to deficiencies in culture conditions that prevent the formation of a stable epidermis [140]. The development of the epidermis relies on the formation of the dermis based on HF inoculation. The epidermis will have trouble forming if the dermis is not well developed prior to HK inoculation. It is possible that samples CoA3, blend, and PCL did not promote the formation of the dermis leading to a poorly formed epidermis and high SEC values. While the difference in SEC values between the coaxial scaffolds

(CoA1, CoA4, and CoA5) were small compared to the gelatin scaffold at day 19 they were significantly different. This may be due to higher levels of dermal growth within the gelatin scaffold.

Ideally, engineered skin should consist of stratified epidermal/dermal layers separated by basement membrane (type IV collagen) with fibroblasts penetrating far into the temporary scaffold. Above the basement membrane would include a basal cell layer and a thick keratinized epidermis. Below the type IV collagen would be fibroblast populated scaffold called the dermis. Epidermal and dermal layers were observed in every scaffold (Figure 4.4). Cell nuclei stained with DAPI were observed to penetrate a significant portion of every scaffold (Figure 4.4). The PCL scaffold showed poor formation of the epidermal constituents and poor penetration of cells into the scaffold. Powell et al. observed the same trend in skin grown on a 100% PCL scaffold [12]. CoA1, CoA3, and CoA5 did not show ideal formation of stratified dermal and epidermal components. The gelatin, blend and CoA4 scaffolds had layers of epidermal and dermal components with evidence of a basal cell layer in each. The engineered skin cultured on scaffold CoA4 showed the most well developed tissue even when compared to the gelatin and blend scaffolds. This shows that the coaxial scaffold CoA4 is capable of supporting the formation of engineered skin and this scaffold is a good candidate for future use as a tissue engineering scaffold.

4.5 Conclusions

Coaxial electrospinning can increase the strength of acellular tissue engineering scaffolds as well as increase the strength of engineered tissue compared with a 100% gelatin scaffold. By increasing the core diameter the strength of the coaxial scaffolds can be controlled without changing scaffold composition or chemistry. It was found that coaxial scaffold CoA4 supported tissue growth similar to gelatin and the blend scaffold and increased the strength of the engineered skin over that grown on gelatin. Coaxial electrospinning could be used in clinical applications to produce high strength tissue engineering scaffolds.

Chapter 5: Conclusions and Recommendations

Electrospinning is an extremely promising method for creating bioactive tissue engineering scaffolds with features that mimic the bodies' natural ECM. Many methods exist to increase the strength of electrospun tissue engineering scaffolds. In this study crosslinking (physical and chemical) and coaxial electrospinning were investigated.

In situ crosslinking via the addition of EDC to a collagen electrospinning solution was a method investigated for reducing scaffold processing time while increasing the strength of the scaffolds. Alone, *in situ* crosslinking failed to stabilize the electrospun collagen in the presence of aqueous media, meaning this specific scaffold could not be used for tissue engineering. Additional crosslinking of this scaffold using DHT treatment stabilized the scaffold in aqueous media and collagenase. The scaffold also had the ability to support fibroblast proliferation, however the scaffold strength and stiffness was significantly lower than scaffolds crosslinked in EDC and ethanol. Therefore *in situ* crosslinking, as presented here, is not suitable for producing scaffolds for tissue engineering where high strength and stiffness are required. Different methods of *in situ* crosslinking should be investigated.

Dehydrothermal crosslinking could be used to stabilize collagen and create a scaffold with increased strength. The processing time is similar to EDC crosslinking with the additional benefit that no chemicals are involved; therefore cytotoxicity is not a factor in DHT treatment. DHT treatment was shown to improve collagen strength and stability

over as-spun collagen although it was also shown to have a lower crosslink density, lower strength, and faster degradation rates than EDC crosslinked collagen. Similarly DHT treatment supported fibroblast infiltration but not as well as EDC crosslinked collagen. DHT treatment could be utilized to produce scaffolds for tissue engineering although the balance of strength, processing time, and degradation rate must be considered for specific applications.

Coaxial electrospinning can be used to engineer the strength and stiffness of a tissue engineering scaffold and the ability to increase the strength of the engineered tissue. Core diameter can easily be controlled by altering solution concentration, core feed rate, and solvent resulting in controllable mechanical properties. In this study it was shown that the scaffolds have varying degrees of stiffness without changes to scaffold architecture or chemistry. These scaffolds could be utilized to assess cellular response to 3D stiffness without confounding factors such as increased crosslinking density, changes in chemistry or time consuming surface modifications. With the inoculation of human dermal fibroblasts and epidermal keratinocytes the coaxial scaffolds promoted cellular growth and proliferation with scaffold CoA4 in particular supporting tissue growth similar to the gelatin control. Coaxial electrospinning could be used in clinical applications to produce high strength tissue engineering scaffolds.

Future investigations involving the version of *in situ* crosslinking presented here, should not be conducted unless a low strength scaffold that has good degradation resistance is required. However, little is known about the chemistry of these scaffolds

which would need to be addressed. Future work could include the investigation of low temperature electrospinning or the use of a different solvent. DHT crosslinking could benefit scaffolds via an additional increase in strength beyond chemical crosslinking methods. For applications where low strength is not an issue and cytotoxicity is a large factor, DHT crosslinking could be applied. Future investigations involving coaxial electrospinning should include the study of shell thickness with a constant core diameter and the influence of shell thickness on the influence of tissue formation. Other investigations involving coaxial electrospinning will include influence of scaffold stiffness in a three dimensional scaffold on cellular behavior and the ability of a synthetic PCL core to modulate the strength and stiffness of electrospun scaffolds *in vivo*.

Master References List

[1] U.S. Department of Health and Human Services: Organ Procurement and Transplantation Network. April 9, 2010. Available from URL: http://optn.transplant.hrsa.gov/data/.

[2] Mayo Clinic. May 12, 2010. Available from URL: http://www.mayoclinic.org/transplant/organ-donation.html.

[3] Pham C, Greenwood J, Cleland H., Woodruff P, Maddern G. Bioengineered skin substitutes for the management of burns: a systematic review. Burns 2007; 33: 946-957.

[4] American Burn Association. May 12, 2010. Available from URL: http://www.ameriburn.org/resources_factsheet.php.

[5] Boyce ST. Design principles for composition and performance of cultured skin substitutes. Burns 2001; 27: 523-533.

[6] Miller SF, Bessey P, Lentz CW, Jeng JC, Schurr M, Browning S. National Burn Repository 2007 Report: A Synopsis of the 2007 Call for Data. Journal of Burn Care and Research 2007; 29: 862-870.

[7] Boyce ST, Warden GD. Principles and practices for treatment of cutaneous wounds with cultured skin substitutes. The American Journal of Surgery 2002; 183: 445-456.

[8] Boyce ST, Kagan RJ, Yakuboff KP, Meyer NA, Rieman MT, Greenhalgh DG, Warden GD. Cultured Skin Substitutes Reduce Donor Skin Harvesting for Closure of Excised Full-Thickness Burns. Annals of Surgery 2002; 235: 269-279.

[9] Bello YM, Falabella AF, Eaglstein WH. Tissue-Engineered Skin: Current Status in Wound Healing. Am J Cln Dermatol 2001; 2: 305-313.

[10] MacNeil S. Progress and opportunities for tissue-engineered skin. Nature 2007; 445: 874-880.

[11] Nguyen DQA, Potokar TS, Price P. An objective long-term evaluation of Integra (a dermal skin substitute) and split thickness skin grafts, in acute burns and reconstructive surgery. Burns 2010; 36: 23-28.

[12] Powell HM, Boyce ST. Engineered Human Skin Fabricated Using Electrospun Collagen-PCL Blends: Morphogenesis and Mechanical Properties. Tissue Engineering 2009; 15: 2177-2187.

[13] L'Heureux N, Pâquet S, Labbé R, Germain L, Auger FA. A completely biological tissue-engineered human blood vessel. FASEB 1998; 12: 47-56.

[14] Badylak SF. Xenogeneic extracellular matrix as a scaffold for tissue reconstruction. Transplant Immunology 2004; 12: 367-377.

[15] Lutolf MP, Hubbell JA. Synthetic biomaterials as instructive extracellular microenvironments for morphogenesis in tissue engineering. Nature Biotechnology 2005; 23: 47-55.

[16] Galbraith CG, Sheetz MP. Forces on adhesive contacts affect cell function. Current Opinion in Cell Biology 1998; 10: 566-571.
[17] Geiger B, Bershadsky A, Pankov R, Yamada KM. Transmembrane extracellular matrix-cytoskeleton crosstalk. Molecular Cell Biology 2001; 2: 793-805.
[18] Thomson RC, Shung AK, Yaszemski MJ, Mikos AG. Polymer Scaffold Processing. In: Lanza RP, Langer R, Vacanti J, editors. Principles of Tissue Engineering. Second Edition. California: Elsevier Science, 2000. p. 251-262.
[19] Zhang R, Ma PX. Poly(A-hydroxyl acids)/hydroxyapatite porous composites for bone-tissue engineering. I. Preparation and morphology. Journal of Biomedical Materials Research 1999; 44: 446-455.
[20] Misra SK, Ansari TI, Valappil SP, Mohn D, Philip SE, Stark WJ, Roy I, Kowles JC, Salih V, Boccaccini AR. Biomaterials 2010; 31: 2806-2815.
[21] Caves JM, Kumar VA, Wen J, Cui WX, Martinez A, Apkarian R, Coats JE, Berland K, Chaikof EL. Fibrillogenesis in Continuously Spun Synthetic Collagen Fiber. Journal of Biomedical Materials Research 2010; 93B: 24-38.
[22] Zeugolis DI, Paul GR, Attenburrow G. Cross-linking of extruded collagen fibers-A biomimetic three-dimensional scaffold for tissue engineering applications. Journal of Biomedical Materials Research 2009; 89: 895-908.
[23] Powell HM, Boyce ST. EDC cross-linking improves skin substitute strength and stability. Biomaterials 2006; 27: 5821-5827.
[24] Drury JL, Mooney DJ. Hydrogels for tissue engineering: scaffold design variables and applications. Biomaterials 2003; 24: 4337-4351.
[25] Ma Z, Kotaki M, Inai R, Ramakrishna S. Potential of Nanofiber Matrix as Tissue-Engineering Scaffolds. Tissue Engineering 2005; 11: 101-113.
[26] Reneker DH, Yarin AL, Fong H, Koombhongse S. Bending instability of electrically charged liquid jets of polymer solutions in electrospinning. Journal of Applied Physics 200; 87: 4531-4547.
[27] Chew SY, Hufnagel TC, Lim CT, Leong KW. Mechanical properties of single electrospun drug-encapsulated nanofibres. Nanotechnology 2006; 17: 3880-3891.
[28] Neotherix. Accessed May 12, 2010. Available at URL: http://www.neotherix.com/technology.php.
[29] Drury JL, Mooney DJ. Hydrogels for tissue engineering: scaffold design variables and applications. Biomaterials 2003; 24: 4337-4351.
[30] Pachence JM, Kohn J. Biodegradable Polymers. In: Lanza RP, Langer R, Vacanti J, editors. Principles of Tissue Engineering. Second Edition. California: Elsevier Science, 2000. p. 263-277.
[31] Barnes CP, Sell SA, Boland ED, Simpson DG, Bowlin GL. Nanofiber technology: Designing the next generation of tissue engineering scaffolds. Advanced Drug Delivery Reviews 2007; 59: 1413-1433.

[32] Li W-J, Laurencin CT, Caterson EJ, Tuan RS, Ko FK. Electrospun nanofibrous structure: a novel scaffold for tissue engineering. Journal of Biomedical Materials Research 2002; 60: 613-621.
[33] Chen J-P, Chang G-Y, Chen J-K. Electrospun collagen/chitosan nanofibrous membrane as wound dressing. Colloids and Surfaces 2008; 313-314: 183-188.
[34] Weadock KS, Miller EJ, Keuffel EL, Dunn MG. Effect of Physical Crosslinking Methods on Collagen-Fiber Durability in Proteolytic Solutions. Journal of Biomedical Materials Research 1996; 32: 221-226.
[35] Li M, Mondrinos MJ, Gandhi MR, Ko FK, Weiss AS, Lelkes PI. Electrospun protein fibers as matrices for tissue engineering. Biomaterials 2005; 26: 5999-6008.
[36] Matthews JA, Wnek GE, Simpson DG, Bowlin GL. Electrospinning of Collagen Nanofibers. Biomacromolecules 2002; 3: 232-238.
[37] McManus MC, Boland ED, Simpson DG, Barnes CP, Bowlin GL. Electrospun fibrinogen: Feasibility as a tissue engineering scaffold in a rat cell culture model. Journal of Biomedical Materials Research 2006; 81A: 299-309.
[38] Zhang YZ, Venugopal J, Huang Z-M, Lim CT, Ramakrishna S. Characterization of the Surface Biocompatibility of the Electrospun PCL-Collagen Nanofibers Using Fibroblasts. Biomacromolecules 2005; 6: 2583-2589.
[39] Powell HM, Supp DM, Boyce ST. Influence of Electrospun Collagen on Wound Contraction of Engineered Skin Substitutes. Biomaterials 2008; 29: 834-843.
[40] Powell HM, Boyce ST. Fiber Density of Electrospun Gelatin Scaffolds Regulates Morphogenesis of Dermal-Epidermal Skin Substitutes. Journal of Biomedical Materials Research 2007; 84: 1078-1086.
[41] Discher DE, Janmey P, Wang Y-L. Tissue Cells Feel and Respond to the Stiffness of their Substrate. Science 2005; 310: 1139-1143.
[42] Pelham RJ, Wang Y-L. Cell locomotion and focal adhesions are regulated by substrate flexibility. Proc. Natl. Acad. Sci. 1997; 94: 13661-13665.
[43] Cortese B, Gigli G, Riehle M. Mechanical Gradient Cues for Guided Cell Motility and Control of Cell Behavior on Uniform Substrates. Adv. Funct. Mater. 2009; 19: 2961-2968.
[44] Lo C-M, Wang H-B, Dembo M, Wang Y-L. Cell Movement is Guided by the Rigidity of the Substrate. Biophysical Journal 2000; 79: 144-152.
[45] Zaari, N., Rajagopalan, P., Kim, S.K., Engler, A.J., and Wong, J.Y. Photopolymerization in Microfluidic Gradient Generators: Microscale Control of Substrate Compliance to Manipulate Cell Response. Advanced Materials 2004; 16: 2133-2137.
[46] Leipzig ND, Shoichet MS. The Effect of Substrate Stiffness on Adult Neural Stem Cell Behavior. Biomaterials 2009; 30: 6867-6878.
[47] Pek YS, Wan AC, Ying JY. The effect of matrix stiffness on mesenchymal stem cell differentiation in a 3D thixotropic gel. Biomaterials 2010; 31: 385-391.

[48] Levy-Mishali M, Zoldan J, Levenberg S. Effect of scaffold stiffness on myoblast differentiation. Tissue Engineering 2009; 15: 935-944.
[49] Collins JM, Ayala P, Desai TA, Russell B. Three-Dimensional Culture with Stiff Microstructures Increases Proliferation and Slows Osteogenic Differentiation of Human Mesenchymal Stem Cells. Small 2010; 6: 355-360.
[50] Chen CS, Mrksich M, Huang S, Whitesides GM, Ingber DE. Geometric control of cell life and death. Science 1997; 276: 1425-1428.
[51] Cornwell KG, Lei P, Andreadis ST, Pins GD. Crosslinking of Discrete Self-Assembled Collagen Threads: Effects on Mechanical Strength and Cell-Matrix Interactions. Journal of Biomedical Materials Research 2006; 80A: 362-371.
[52] Yannas IV, Burke JF, Orgill DP, Skrabut EM. Wound Tissue Can Utilize a Polymeric Template to Synthesize a Functional Extension of Skin. Science 1982; 215: 174-176.
[53] Park S-N, Park J-C, Kim HO, Song MJ, Suh H. Characterization of porous collagen/hyaluronic acid scaffold modified by 1-ethyl-3-(3-dimethylaminopropyl)carbodiimide cross-linking. Biomaterials 2002; 23: 1205-1212.
[54] Powell HM, McFarland KL, Butler DL, Supp DM, Boyce ST. Uniaxial strain regulates gene expression, morphogenesis and tissue strength in engineered skin. Tissue Engineering Part A 2010; 16: 1083-1092.
[55] Olde Damink LHH, Dijkstra PJ, van Luyn MJA, van Wachem PB, Nieuwenhuis P, Feijen J. Glutaraldehyde as a crosslinking agent for collagen-based biomaterials. Journal of Materials Science: Materials in Medicine 1995; 6: 460-472.
[56] Harley BA, Leung JH, Silva ECCM, Gibson LJ. Mechanical characterization of collagen-glycosaminoglycan scaffolds. Acta Biomaterialia 2007; 3: 463-474.
[57] Bellincampi LD, Dunn MG. Effect of Crosslinking Method on Collagen Fiber-Fibroblast Interactions. Journal of Applied Polymer Science 1997; 63: 1493-1498.
[58] Torres-Giner S, Gimeno-Alcaniz JV, Ocio MJ, Lagaron JM. Comparative Performance of Electrospun Collagen Nanofibers Cross-linked by Means of Different Methods. American Chemical Society: Applied Materials and Interfaces 2009; 1: 218-223.
[59] Pieper JS, Oosterhof A, Dijkstra PJ, Veerkamp JH, van Kuppevelt TH. Preparation and Characterization of Porous Crosslinked Collagenous Matrices Containing Bioavailable Chondroitin Sulphate. Biomaterials 1999; 20: 847-858.
[60] Haugh MG, Jaasma MJ, O'Brien FJ. The Effect of Dehydrothermal Treatment on the Mechanical and Structural Properties of Collagen-GAG Scaffolds. Journal of Biomedical Materials Research 2009; 89: 363-369.
[61] Scotchford CA, Cascone MG, Downes S, Giusti P. Osteoblast Responses to Collagen-PVA Bioartificial Polymers In Vitro: the Effects of Cross-linking Method and Collagen Content. Biomaterials 1998; 19: 1-11.

[62] Xiang Z, Liao R, Kelly MS, and Spector M. Collagen-GAG Scaffolds Grafted onto Myocardial Infarcts in a Rat Model: A Delivery Vehicle for Mesenchymal Stem Cells. Tissue Engineering 2006; 12: 2467-2478.
[63] Marzec E, Pietrucha K. The Effect of Different Methods of Cross-linking of Collagen on its Dielectric Properties. Biophysical Chemistry 2008; 132: 89-96.
[64] Ma L, Gao C, Mao Z, Shen J, Hu X, Han C. Thermal Dehydration Treatment and Glutaraldehyde Cross-linking to Increase the Biostability of Collagen-Chitosan Porous Scaffolds Used as Dermal Equivalent. Journal of Biomaterials Science 2003; 14: 861-874.
[65] Lee CR, Grodzinsky AJ, and Spector M. The Effects of Cross-linking of Collagen-Glycosaminoglycan Scaffolds on Compressive Stiffness, Chondrocyte-Mediated Contraction, Proliferation and Biosynthesis. Biomaterials 2001; 22: 3145-3154.
[66] Yannas TV, Tobolsky AV. Cross-linking of Gelatine by Dehydration. Nature 1967; 215: 509-510.
[67] Boland ED, Matthews JA, Pawlowski KJ, Simpson DG, Wnek GE, Bowlin GL. Electrospinning Collagen and Elastin: Preliminary Vascular Tissue Engineering. Frontiers in Bioscience 2004; 9: 1422-1432.
[68] Yeo I-S, Oh J-E, Jeong L, Lee TS, Lee SL, Park WH, Min B-M. Collagen-Based Biomimetic Nanofibrous Scaffolds: Preparation and Characterization of Collagen/Silk Fibroin Bicomponent Nanofibrous Structures. Biomacromolecules 2008; 9: 1106-1116.
[69] Dong B, Arnoult O, Smith ME, Wnek GE. Electrospinning of Collagen Nanofiber Scaffolds from Benign Solvents. Macromolecular Rapid Communications 2009; 30: 539-542.
[70] Khor E. Methods for the Treatment of Collagenous Tissues for Bioprostheses. Biomaterials 1997; 18: 95-105.
[71] Jarman-Smith ML, Bodamyali T, Stevens C, Howell JA, Horrocks M, Chaudhuri JB. Porcine Collagen Crosslinking, Degradation and its Capability for Fibroblast Adhesion and Proliferation. Journal of Materials Science: Materials in Medicine 2004; 15: 925-932.
[72] Wessels QB, Pretorius E. Enhanced Stabilization of Collagen-Based Dermal Regeneration Scaffolds Through the Combination of Physical and Chemical Crosslinking. South African Journal of Science 2008; 104: 513-516.
[73] Buttafoco L, Kolkman NG, Engbers-Buijtenhuijs P, Poot AA, Dijkstra PJ, Vermes I, Feijen J. Electrospinning of Collagen and Elastin for Tissue Engineering Applications. Biomaterials 2006; 27: 724-734.
[74] Song J-H, Kim H-E, Kim H-W. Electrospun Fibrous Web of Collagen-Apatite Precipitated Nanocomposite for Bone Regeneration. Journal of Materials Science: Materials in Medicine 2008; 19: 2925-2932.

[75] Cao H, Xu S-Y. EDC/NHS-Crosslinked Type II Collagen-Chondroitin Sulfate: Characterization and In Vitro Evaluation. Journal of Materials Science: Materials in Medicine 2008; 19: 567-575.
[76] Zeugolis DI, Paul GR, Attenburrow G. Cross-linking of Extruded Collagen Fibers-A Biomimetic Three-dimensional Scaffold for Tissue Engineering Applications. Journal of Biomedical Materials Research 2009; 89A: 895-908.
[77] Everaerts F, Torrianni M, Hendriks M, Feijen J. Biomechanical Properties of Carbodiimide Crosslinked Collagen: Influence of the Formation of Ester Crosslinks. Journal of Biomedical Materials Research 2007; 85A: 547-555.
[78] Powell HM, Boyce ST. Engineered human skin fabricated using electrospun collagen-PCL blends: morphogenesis and mechanical properties. Tissue Engineering 2009; 15: 2177-2187.
[79] Khor HL, Ng KW, Schantz JT, Phan T-T, Lim TC, Teoh SH, Hutmacher DW. Poly(ε-caprolactone) films as a potential substrate for tissue engineering an epidermal equivalent. Materials Science and Engineering 2002; 20: 71-75.
[80] Venugopal J, Zhang YZ, Ramakrishna S. Fabrication of modified and functionalized polycaprolactone nanofibre scaffolds for vascular tissue engineering. Nanotechnology 2005; 16: 2138-2142.
[81] Wu L, Li H, Li S, Li X Yuan X, Li X, Zhang Y. Composite fibrous membranes of PLGA and chitosan prepared by coelectrospinning and coaxial electrospinning. Journal of Biomedical Materials Research 2010; 92: 563-574.
[82] Heydarkhan-Hagvall S, Schenke-Layland K, Dhanasopon AP, Rofail F, Smith H, Wu BM, Shemin R, Beygui RE, MacLellan WR. Three-dimensional electrospun ECM-based hybrid scaffolds for cardiovascular tissue engineering. Biomaterials 2008; 29: 2907-2914.
[83] Lee J-J, Yu H-S, Hong S-J, Jeong I, Jang J-H, Kim H-W. Nanofibrous membrane of collagen-polycaprolactone for cell growth and tissue regeneration. Journal of Materials Science: Materials in Medicine 2009; 20: 1927-1935.
[84] Schnell E, Klinkhammer K, Balzer S, Brook G, Klee D, Dalton P, Mey J. Guidance of glial cell migration and axonal growth on electrospun nanofiber of poly-ε-caprolactone and a collagen/ poly-ε-caprolactone blend. Biomaterials 2007; 28: 3012-3025.
[85] Duan Y, Wang Z, Yan W, Wang S, Zhang S, Jia J. Preparation of collagen-coated electrospun nanofibers by remote plasma treatment and their biological properties. Journal of Biomaterials Science Polymer Edition 2007; 18: 1153-1164.
[86] He W, Ma Z, Yong T, Teo WE, Ramakrishna S. Fabrication of collagen-coated biodegradable polymer nanofiber mesh and its potential for endothelial cells growth. Biomaterials 2005; 26: 7606-7615.
[87] Sun Z, Zussman E, Yarin AL, Wendorff JH, Greiner A. Compound Core-Shell Polymer Nanofibers by Co-Electrospinning. Advanced Materials 2003; 15: 1929-1932.

[88] Jiang H, Hu Y, Li Y, Zhao P, Zhu K, Chen W. A facile technique to prepare biodegradable coaxial electrospun nanofibers for controlled release of bioactive agents. Journal of Controlled Release 2005; 108: 237-243.
[89] Saraf A, Lozier G, Haesslein A, Kasper K, Raphael RM, Baggett LS, Mikos AG. Fabrication of Nonwoven Coaxial Fiber Meshes by Electrospinning. Tissue engineering 2009; 15: 333-344.
[90] Han D, Boyce ST, Steckl AJ. Versatile Core-Sheath Biofibers using Coaxial Electrospinning. Materials Research Society 2008; 1094: 1-6.
[91] Chen R, Li XQ, Ke QF, He CL, Mo XM. Fabrication and characterization of collagen (shell)/thermoplastic polyurethane (core) composite nanofibers by coaxial electrospinning. E-Polymers 2010; 009: 1-8.
[92] Huang Z-M, Zhang Y, Ramakrishna S. Double-Layered Composite Nanofibers and Their Mechanical Performance. Journal of Polymer Science 2005; 43: 2852-2861.
[93] Chen S, Hou H, Hu P, Wendorff JH, Greiner A, Agarwal S. Polymeric Nanosprings by Bicomponent Electrospinning. Macromolecular Materials and Engineering 2009; 294: 265-271.
[94] Zhang Y, Huang Z-M, Xu X, Lim CT, Ramakrishna S. Preparation of Core-Shell Structured PCL-r-Gelatin Bi-Component Nanofibers by Coaxial Electrospinning. Chemistry of Materials 2004; 16: 3406-3409.
[95] Lannutti J, Reneker D, Ma T, Tomasko D, Farson D. Electrospinning for tissue engineering scaffolds. Materials Science and Engineering 2007; C27: 504-509.
[96] Liang D, Hsaio B, Chu B. Functional electrospun nanofibrous scaffolds for biomedical applications. Advances in Drug Delivery Reviews 2007; 59: 1392-1412.
[97] Lu H, Chen WJ, Xing Y, Ying DJ. Design and preparation of an electrospun biomaterials surgical patch. Journal of Bioactive and Compatible Polymers 2009; 24: 158-168.
[98] Wray LS, Orwin EJ. Recreating the microenvironment of the native cornea for tissue engineering applications. Tissue Engineering 2009; 15: 1463-1472.
[99] Ma L, Gao C, Mao Z, Shen J, Hu X, Han C. Thermal dehydration treatment and glutaraldehyde cross-linking to increase the biostability of collagen-chitosan porous scaffolds used as dermal equivalent. Journal of Biomaterials Science 2003; 14: 861-874.
[100] Schiffman JD, Schauer CL. One-step electrospinning of cross-linked chitosan fibers. Biomacromolecules 2007; 8: 2665-2667.
[101] Ma Y, Agarwal US, Vekemans JAJM, Sikkema DJ. NMR based determination of minute acid functionality: end-groups in PET. Polymer 2003; 44: 4429-4434.
[102] Kurzer K, Zadeh D. Advances in the chemistry of carbodiimides. Chemical Reviews 1967; 67: 107-152.

[103] Billiar K, Murray J, Laude D, Abraham G, Bachrach N. Effects of carbodiimide crosslinking conditions on the physical properties of laminated intestinal submucosa. Journal of Biomedical Materials Research 2001; 56A: 101-108.
[104] Pulieri E, Chiono V, Ciardelli G, Vozzi G, Ahluwalia A, Domenici C, Vozzi F, Giusti P. Chitosan/gelatin blends for biomedical applications. Journal of Biomedical Materials Research 2008; 86: 311-322.
[105] Ber S, Kose GT, Hasirci V. Bone tissue engineering on patterned collagen films: an in vitro study. Biomaterials 2005; 26: 1977-1986.
[106] Wells RG. The roll of matrix stiffness in regulating cell behavior. Hepatology 2008; 47: 1394-1400.
[107] Subramanian, A. and Lin, H.Y. Crosslinked Chitosan: Its Physical Properties and the Effects of Matrix Stiffness on Chondrocyte Cell Morphology and Proliferation. Journal of Biomedical Materials Research 2005; 75A: 742-753.
[108] Leipzig ND, Shoichet MS. The effect of substrate stiffness on adult neural stem cell behavior. Biomaterials 2009; 30: 6867-6878.
[109] Zaari N, Rajagopalan P, Kim SK, Engler AJ, Wong JY. Photopolymerization in Microfluidic Gradient Generators: Microscale Control of Substrate Compliance to Manipulate Cell Response. Advanced Materials 2004; 16: 2133-2137.
[110] Dikovsky D, Bianco-Peled H, Seliktar D. Defining the role of matrix compliance and proteolysis in three-dimensional cell spreading and remodeling. Biophysical Journal 2008; 94: 2914-2925.
[111] Balguid A, Mol A, van Marion MH, Bank RA, Bouten CVC, Baaijens FPT. Tailoring Fiber Diameter in Electrospun Polycaprolactone Scaffolds for Optimal Cellular Infiltration in Cardiovascular Tissue Engineering. Tissue Engineering 2009; 15: 437-444.
[112] Jacobs V, Anandjiwala RD, Maaza M. The influence of Electrospinning Parameters on the structural morphology and diameter of electrospun nanofibers. Journal of Applied Polymer Science 2010; 115: 3130-3136.
[113] Chen M, Patra PK, Warner SB, Bhowmick S. Role of fiber diameter in adhesion and proliferation of NIH 3T3 fibroblast on electrospun polycaprolactone scaffolds. Tissue Engineering 2007; 13: 579-587.
[114] Deitzel JM, Kleinmeyer J, Harris D, Tan NCB. The effect of processing variables on the morphology of electrospun nanofibers and textiles. Polymer 2001; 42: 261-272.
[115] Shawon J, Sung C. Electrospinning of polycarbonate nanofibers with solvent mixtures THF and DMF. Journal of Materials Science 2004; 39: 4605-4613.
[116] Lee KH, Kim HY, La YM, Lee DR, Sung NH. Influence of a Mixing Solvent with Tetrahydrofuran and N,N-Dimethylformamide on Electrospun Poly(vinyl chloride) Nonwoven Mats. Journal of Polymer Science 2002; 40: 2259-2268.
[117] Koombhongse, S., Liu, W. and Reneker, D.H. Flat Polymer Ribbons and Other Shapes by Electrospinning. Journal of Polymer Science 2001; 39: 2598-2606.

[118] Soliman S, Pagliari S, Rinaldi A, Forte G, Fiaccavento R, Pagliari F, Franzese O, Minieri M, Nardo PD, Licoccia S, Traversa E. Multiscale three-dimensional scaffolds for soft tissue engineering via multimodal electrospinning. Acta Biomaterialia 2010; 6: 1227-1237.
[119] Han D, Boyce ST, Steckl AJ. Versatile Core-Sheath Biofibers using Coaxial Electrospinning. Materials Research Society 2008; 1094: 1-6.
[120] Medical Care Guide. Burn Survivor Resource Center. Journal of Burn Care and Rehabilitation, 2008.
[121] American Burn Association National Burn Repository 2005 Report.
[122] Ressner RA, Murray CK, Griffith ME, Rasnake MS, Hospenthal DR, Wolf SE. Outcomes of bacteremia in burn patients involved in combat operations overseas. Journal of the American College of Surgeons 2008; 206: 439-444.
[123] Rose J, Herndon D. Advances in the treatment of burn patients. Burns 1997; 23: S19-S26.
[124] Herndon DN, Barrow RE, Rutan RL, et al. A comparison of conservative versus early excision. Therapies in severely burned patients. Annals of Surgery 1989; 209: 547-552.
[125] Fratianne R, Brandt C. Improved survival of adults with extensive burns. Journal of Burn Care and Rehabilitation 1997; 18: 347-351.
[126] Sheridan RL, Remensnyder JP, Schnitzer JJ, Schulz JT, Ryan CM, Tompkins RG. Current expectations for survival in pediatric burns. Archives of Adolescent and Pediatric Medicine 2000; 154: 245-249.
[127] Berthod F, Damour O. In vitro reconstructed skin models for wound coverage in deep burns. British Journal of Dermatology 1997; 136: 809-816.
[128] Bello YM, Falabella AF, Eaglstein WH. Tissue-Engineered Skin: Current Status in Wound Healing. American Journal of Clinical Dermatology 2001; 2:305-313.
[129] Ehrenreich M, Ruszczak Z. Update on tissue-engineered biological dressings. Tissue Engineering 2006; 12: 2407-2424.
[130] Heimbach D, Lutterman A, Burke J, Cram A, Herndon D, Hunt J, Jordan M, McManus W, Solem L, Warden G, Zawacki B. Artificial dermis for major burn: A multi-center randomized clinical trial. Annals of Surgery 1988; 208: 313-320.
[131] Boyce ST, Christianson DJ, Hansbrough JF. Structure of collagen-GAG dermal skin substitute optimized for cultured human epidermal keratinocytes. Journal of Biomedical Materials Research 1988; 22:939-957.
[132] Eaglstein WH, Alvarez OM, Auletta M, Leffel D, Rogers GS, Zitelli JA, Norris JEC, Thomas I, Irondo M, Fewkes J, Hardin-Young J, Duff RG, Sabolinski ML. Acute excisional wounds treated with a tissue-engineered skin (Apligraf). Dermatology Surgery 1999; 25: 195-201.
[133] Clark JA, Cheng JCY, Leung KS. Mechanical properties of normal skin and hypertrophic scars. Burns 1996; 22: 443-446.

[134] Boyce ST, Kagan RJ, Greenhalgh DG, Warner P, Yakuboff KP, Palmieri T, Warden GD. Cultured skin substitutes reduce requirements for harvesting of skin autograft for closure of excised, full-thickness burns. Journal of Trauma-Injury, Infection and Critical Care 2006; 60253: 821-829.
[135] Boyce ST, Goretsky M, Greenhalgh DG, Kagan RJ, Rieman MT, Warden GD. Comparative assessment of cultured skin substitutes and native skin autograft for treatment of full-thickness burns. Annals of Surgery 1995; 222: 743-752.
[136] Ekaputra AK, Zhou Y, Cool SM, Hutmacher DW. Composite electrospun scaffolds for engineering tubular bone grafts. Tissue Engineering 2009; 15A: 3779-3788.
[137] Zhao P, Jiang H, Pan H, Zhu K, Chen W. Biodegradable fibrous scaffolds composed of gelatin coated poly(ε-caprolactone) prepared by coaxial electrospinning. Journal of Biomedical Materials Research 2007; 83A: 372-382.
[138] Wu L, Li H, Li S, Li X, Yuan X, Li X, Zhang Y. Composite fibrous membranes of PLGA and chitosan prepared by coelectrospinning and coaxial electrospinning. Journal of Biomedical Materials Research 2010; 92A: 563-574.
[139] Venugopal JR, Zhang Y, Ramakrishna S. In vitro culture of human dermal fibroblasts on electrospun polycaprolactone collagen nanofibrous membrane. Artificial Organs 2006; 30: 440-446.
[140] Boyce ST, Supp AP, Harriger MD, Pickens WL, Wickett RR, Hoath SB. Surface electrical capacitance as a noninvasive index of epidermal barrier in cultured skin substitutes in athymic mice. Journal of Investigative Dermatology 1996; 107: 82-87.